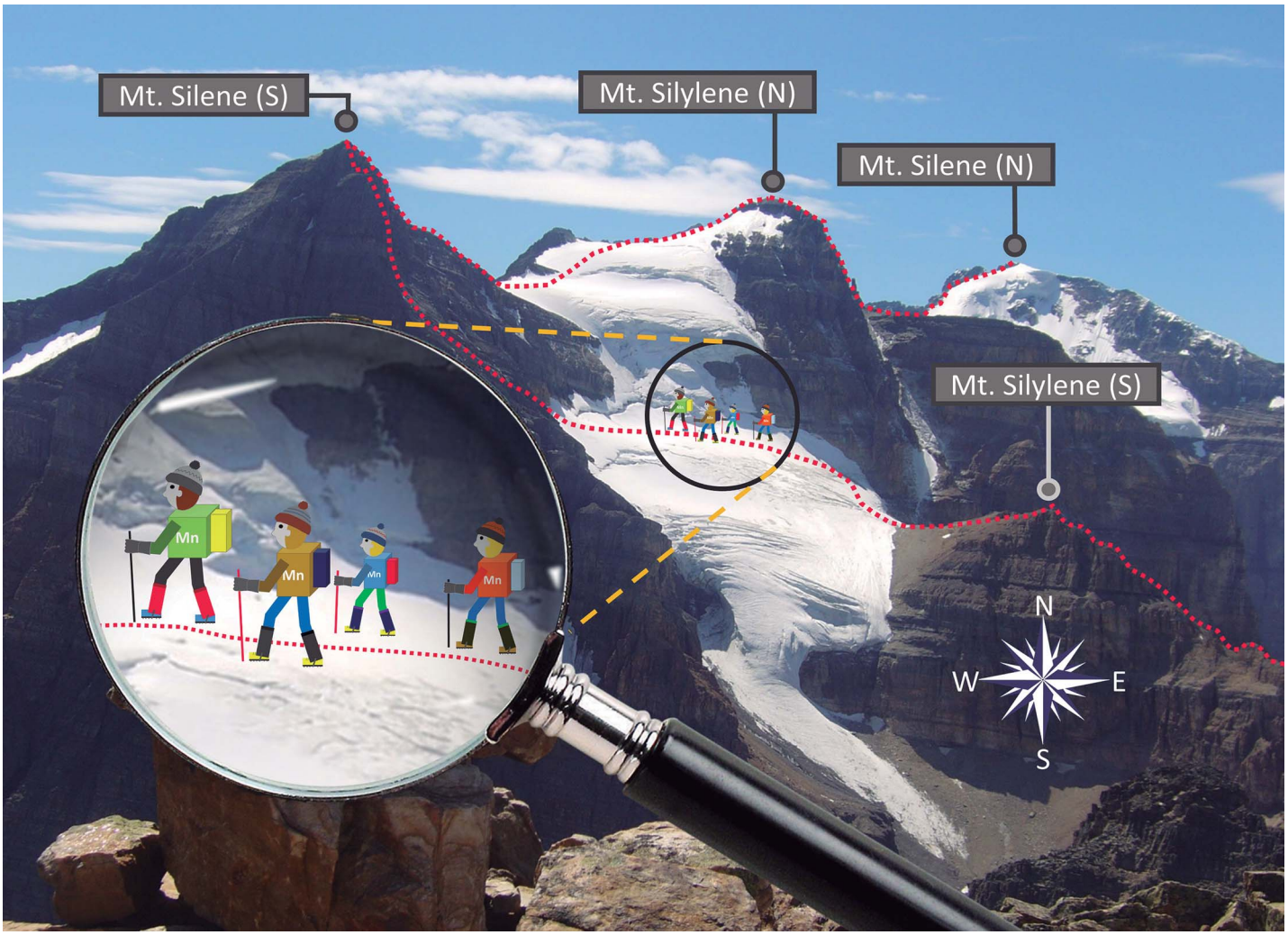

Showcasing research from Professor Emslie's laboratory, Department of Chemistry, McMaster University, Hamilton, Ontario, Canada.

Interconversion and reactivity of manganese silyl, silylene, and silene complexes

This work involves the reaction of a monosubstituted manganese silylene complex ($L_xHMn{=}SiHR$) with ethylene to afford the first transition metal silene complex with an Si*H* substituent ($L_xHMn(RHSi{=}CHMe)$), unprecedented isomerization to a silylene isomer ($L_xHMn{=}SiEtR$), and further reaction with ethylene to afford a new silene complex ($L_xHMn(REtSi{=}CHMe)$). Reaction mechanisms were elucidated through reactions with C_2D_4, and we report the involvement of the aforementioned silene complexes in catalytic ethylene hydrosilylation. The image shows Mn atoms traversing 4 mountain peaks representing the stepwise silylene → silene → silylene → silene transformations in the research.

As featured in:

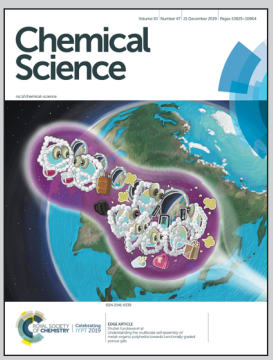

See Jeffrey S. Price and David J. H. Emslie, *Chem. Sci.*, 2019, **10**, 10853.

ROYAL SOCIETY OF CHEMISTRY | Celebrating IYPT 2019

rsc.li/chemical-science

Registered charity number: 207890

Chemical Science

EDGE ARTICLE

View Article Online
View Journal | View Issue

Cite this: *Chem. Sci.*, 2019, **10**, 10853

All publication charges for this article have been paid for by the Royal Society of Chemistry

Interconversion and reactivity of manganese silyl, silylene, and silene complexes†

Jeffrey S. Price and David J. H. Emslie *

Manganese disilyl hydride complexes [(dmpe)$_2$MnH(SiH$_2$R)$_2$] (**4^{Ph}**: R = Ph, **4^{Bu}**: R = ^{n}Bu) reacted with ethylene to form silene hydride complexes [(dmpe)$_2$MnH(RHSi=CHMe)] (**6^{Ph,H}**: R = Ph, **6^{Bu,H}**: R = ^{n}Bu). Compounds **6^{R,H}** reacted with a second equivalent of ethylene to generate [(dmpe)$_2$MnH(REtSi=CHMe)] (**6^{Ph,Et}**: R = Ph, **6^{Bu,Et}**: R = ^{n}Bu), resulting from apparent ethylene insertion into the silene Si–H bond. Furthermore, in the absence of ethylene, silene complex **6^{Bu,H}** slowly isomerized to the silylene hydride complex [(dmpe)$_2$MnH(=SiEt^{n}Bu)] (**3^{Bu,Et}**). Reactions of **4^R** with ethylene likely proceed *via* low-coordinate silyl {[(dmpe)$_2$Mn(SiH$_2$R)] (**2^{Ph}**: R = Ph, **2^{Bu}**: R = ^{n}Bu)} or silylene hydride {[(dmpe)$_2$MnH(=SiHR)] (**3^{Ph,H}**: R = Ph, **3^{Bu,H}**: R = ^{n}Bu)} intermediates accessed from **4^R** by H$_3$SiR elimination. DFT calculations and high temperature NMR spectra support the accessibility of these intermediates, and reactions of **4^R** with isonitriles or N-heterocyclic carbenes yielded the silyl isonitrile complexes [(dmpe)$_2$Mn(SiH$_2$R)(CNR′)] (**7a–d**: R = Ph or ^{n}Bu; R′ = *o*-xylyl or ^{t}Bu), and NHC-stabilized silylene hydride complexes [(dmpe)$_2$MnH{=SiHR(NHC)}] (**8a–d**: R = Ph or ^{n}Bu; NHC = 1,3-diisopropylimidazolin-2-ylidene or 1,3,4,5-tetramethyl-4-imidazolin-2-ylidene), respectively, all of which were crystallographically characterized. Silyl, silylene and silene complexes in this work were accessed *via* reactions of [(dmpe)$_2$MnH(C$_2$H$_4$)] (**1**) with hydrosilanes, in some cases followed by ethylene. Therefore, ethylene (C$_2$H$_4$ and C$_2$D$_4$) hydrosilylation was investigated using [(dmpe)$_2$MnH(C$_2$H$_4$)] (**1**) as a pre-catalyst, resulting in stepwise conversion of primary to secondary to tertiary hydrosilanes. Various catalytically active manganese-containing species were observed during catalysis, including silylene and silene complexes, and a catalytic cycle is proposed.

Received 7th September 2019
Accepted 23rd October 2019

DOI: 10.1039/c9sc04513a

rsc.li/chemical-science

Introduction

Silylenes (:SiR$_2$)[1,2] and silenes (R$_2$C=SiR$_2$),[2–4] heavy analogues of carbenes and alkenes, are highly reactive species, and in the absence of extremely bulky or π-donor substituents,[5] transition metal coordination is required for stabilization.[3,6–8] However, complexes bearing unstabilized *silylene* ligands are involved in various catalytic processes involving silanes, including dehydrocoupling, substituent redistribution, hydrosilylation, and the Direct process for silane chlorination.[7] Similarly, *silene* complexes have in several instances been hypothesized to play an important role in catalysis, typically on the basis of indirect observations. For example, they are thought to be active species in polycarbosilane synthesis from dichloromethylsilanes and sodium in the presence of [Cp$_2$ZrCl$_2$],[9] dehydrogenative coupling of HSiMe$_3$ by [(Me$_3$P)$_3$RuH$_3$(SiMe$_3$)],[10] transfer dehydrogenative coupling of HSiEt$_3$ catalysed by [(*p*-cymene)RuH$_2$(SiEt$_3$)$_2$] or [Cp*RhH$_2$(SiEt$_3$)$_2$],[11] and trialkylsilane (*e.g.* HSiMe$_3$) perdeuteration catalysed by [(Me$_3$P)$_4$OsH(SiMe$_3$)][12] or [(C$_6$Me$_6$)RuH$_2$(SiMe$_3$)$_2$][13] in C$_6$D$_6$. Furthermore, silene complexes were recently proposed as off-cycle species in sila-heterocycle synthesis by intramolecular silylation of primary C–H bonds,[14] and free silenes play a key role in hot wire CVD of SiC using alkylsilanes.[15]

Early examples of isolable transition metal complexes bearing a terminal *silylene* ligand featured Lewis base coordination to silicon,[16] and base-free terminal silylene complexes were not isolated until 1990.[17] Since then, a range of such complexes have been reported; almost exclusively mid- and late-transition metal complexes,[18] which are electrophilic at silicon. By contrast, silylene complexes with an Si*H* substituent remain relatively rare; the first example, [(Et$_3$P)$_3$IrH$_2${=SiH(C$_6$H$_3$-Mes$_2$-2,6)}][B(C$_6$F$_5$)$_4$], was reported in 2002,[19] and in the same year, Tilley *et al.* suggested [{PhB(CH$_2$PPh$_2$)$_3$}IrH$_2${=SiH(Trip)}] as an intermediate in the synthesis of [{PhB(CH$_2$PPh$_2$)$_3$}IrH$_2${=Si(C$_8$H$_{15}$)(Trip)}].[20] Two years later, the Tobita[21] and Tilley[22] groups independently reported the first structurally characterized examples,

Department of Chemistry, McMaster University, 1280 Main Street West, Hamilton, Ontario, L8S 4M1, Canada. E-mail: emslied@mcmaster.ca

† Electronic supplementary information (ESI) available: Experimental procedures, NMR frequencies and selected NMR spectra for complexes and hydrosilylation products, tabulated bonding parameters from X-ray structures, computational results (tables of bonding parameters, bond orders, energies, and Hirshfeld charges), visualization of calculated structures, and tables of crystal data/crystal structure refinement (PDF). Cartesian coordinates of the calculated structures (*XYZ*). CCDC 1946403–1946410. For ESI and crystallographic data in CIF or other electronic format see DOI: 10.1039/c9sc04513a

$[(C_5Me_4Et)(OC)_2WH(=SiH\{C(SiMe_3)_3\})]$ and $[Cp^*(dmpe)MoH(=SiHPh)]$, respectively. Base-free $L_xM{=}SiHR$ complexes have only been isolated for groups 6, 8 and 9,[19–26] and group 7 examples are notably absent. Extensive studies by the Tilley and Tobita groups have demonstrated that hydrogen substituents on the sp^2 Si centers permit these silylene complexes to demonstrate unusual reactivity, including alkene insertion into the silylene Si–H bond in cationic complexes, and conversion to silylyne (M≡SiR) complexes.[20,23,25]

A small number of transition metal *silene* complexes have also been isolated, with 2nd and 3rd row transition metal examples (bearing sterically and electronically unstabilized silene ligands)[27] limited to complexes of Ir, Ru, and W (Fig. 1).[28–30] Furthermore, outside of our recent report of manganese silene complexes (*vide infra*), first row transition metal complexes bearing unstabilized silene ligands have not been isolated.

We recently communicated the synthesis (Scheme 1) of the first unstabilized terminal silylene complexes of a group 7 metal, $[(dmpe)_2MnH(=SiR_2)]$ ($\mathbf{3^{Ph2}}$: R = Ph, $\mathbf{3^{Et2}}$: R = Et), by the reaction of $[(dmpe)_2MnH(C_2H_4)]$ (**1**)[31] with secondary hydrosilanes (H_2SiR_2).[32] In the solid state, the silylene and hydride ligands are *cis* (diphenyl analogue $\mathbf{3^{Ph2}}$) or *trans* (diethyl analogue $\mathbf{3^{Et2}}$) disposed, in the former case with an Si–H interligand interaction. Silylene hydride complexes with interligand Si–H interactions were first reported in 2004 by the Tobita[21] ($[(C_5Me_4Et)(OC)_2WH(=SiH\{C(SiMe_3)_3\})]$) and Tilley[22] ($[Cp^*(dmpe)MoH(=SiEt_2)]$)[33] groups, and since that time, W, Fe, Ru, and Ni examples have been reported.[25,26,34] Uniquely, the *cis* and *trans* isomers of $\mathbf{3^{Ph2}}$ exist in equilibrium with one another in solution (Scheme 1).

In contrast to the reactions of **1** with secondary hydrosilanes, reactions with primary hydrosilanes (H_3SiR) yielded disilyl hydride complexes $[(dmpe)_2MnH(SiH_2R)_2]$ ($\mathbf{4^{Ph}}$: R = Ph, $\mathbf{4^{Bu}}$: R = ^{n}Bu; Scheme 1).[35] The syntheses of both silylene hydride complexes $\mathbf{3^{R2}}$ and disilyl hydride complexes $\mathbf{4^{R}}$ from **1** were proposed to proceed *via* a 5-coordinate silyl intermediate $[(dmpe)_2Mn(SiHRR')]$ ($\mathbf{2^{Ph2}}$: R = R′ = Ph; $\mathbf{2^{Et2}}$: R = R′ = Et; $\mathbf{2^{Ph}}$: R = Ph, R′ = H; $\mathbf{2^{Bu}}$: R = ^{n}Bu, R′ = H), which undergoes α-hydride elimination to generate $\mathbf{3^{R2}}$, or oxidative addition of a second equivalent of hydrosilane to afford $\mathbf{4^{R}}$ (Scheme 1).

Reactions of the silylene hydride complexes with ethylene generated the silene hydride complexes *cis*-$[(dmpe)_2MnH(R_2Si{=}CHMe)]$ {R = Ph ($\mathbf{6^{Ph2}}$) or Et ($\mathbf{6^{Et2}}$); Scheme 1}. This type of silylene to silene transformation is unprecedented, although Tilley *et al.* have reported conversion of $[Cp^*(Me_3P)Ir(Me)(=SiMe_2)]^+$ to the silene hydride isomer, $[Cp^*(Me_3P)IrH(Me_2Si{=}CH_2)]^+$.[28] The intermediacy of a trimethylsilyl iridium complex in this reaction was supported by trapping reactions with CO and ethylene. Additionally, the iridium silene hydride cation reacted with pyridine to afford $[Cp^*(Me_3P)Ir(Me)\{=SiMe_2(py)\}]^+$, highlighting the reversibility of the silylene–silene transformation (Scheme 2).[28] Furthermore, many of the known silene complexes were synthesized by installation of a CH_2SiR_2H (R = Me or Ph) or SiR_2Me group, followed by β-hydride elimination.[14,28,29] These classes of reaction are combined in Scheme 2, highlighting the potential to interconvert between silylene, silyl, silene, and alkyl (CH_2SiHR_2) complexes.

Both silylene hydride complexes $\mathbf{3^{R2}}$ and disilyl hydride complexes $\mathbf{4^{R}}$ have been shown to react with H_2 (Scheme 1) to

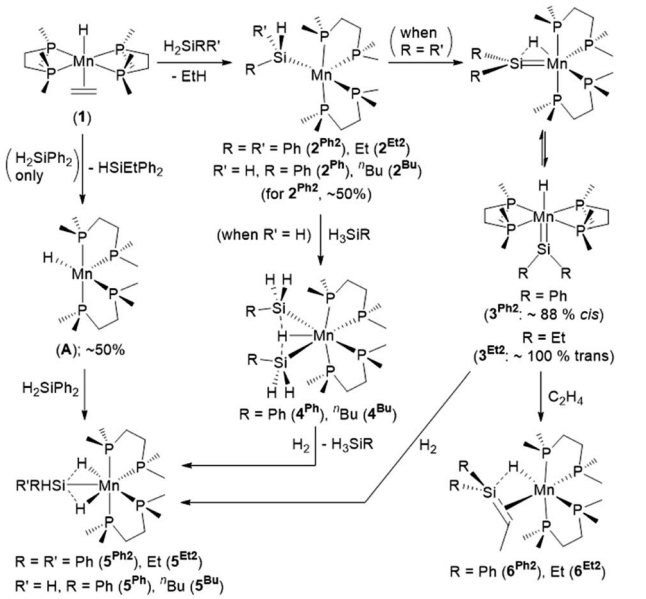

Scheme 1 Reactions of $[(dmpe)_2MnH(C_2H_4)]$ (**1**) with primary and secondary hydrosilanes to generate silylene-hydride ($\mathbf{3^{R2}}$) and disilyl hydride ($\mathbf{4^{R}}$) complexes respectively, reactions of the latter two complexes with H_2 to generate isostructural silyl dihydride complexes ($\mathbf{5^{R2}}$ or $\mathbf{5^{R}}$ respectively), and reaction of silylene hydride complexes $\mathbf{3^{R2}}$ with ethylene to generate silene hydride complexes ($\mathbf{6^{R2}}$).[32,35,36] Only one isomer is shown for **2**, **5**, and **A**.

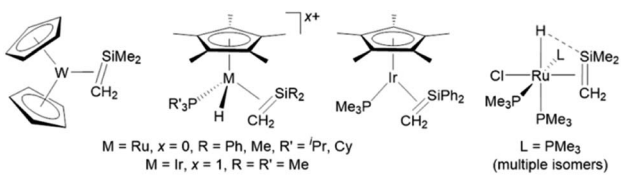

Fig. 1 Second and third row transition metal complexes bearing sterically and electronically unstabilized silene ligands.

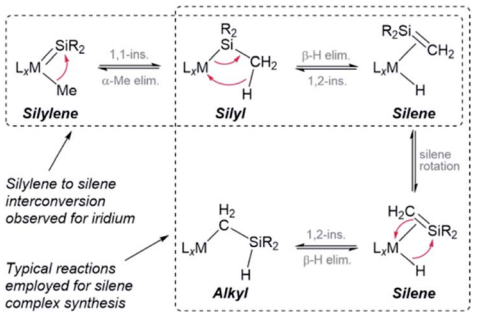

Scheme 2 Reported reactions capable of converting between silylene, silyl, silene and alkyl isomers. Electron pushing arrows are shown for the forward direction.

generate silyl dihydride complexes [(dmpe)$_2$MnH$_2$(SiHRR′)] ($\mathbf{5^{Ph2}}$: R = R′ = Ph; $\mathbf{5^{Et2}}$: R = R′ = Et; $\mathbf{5^{Ph}}$: R = Ph, R′ = H; $\mathbf{5^{Bu}}$: R = ^{n}Bu, R′ = H), suggesting the accessibility of a common low-coordinate silyl intermediate, [(dmpe)$_2$Mn(SiHRR′)] (**2**).[32,36] Therefore, disilyl hydride complexes $\mathbf{4^R}$ could potentially react as sources of manganese silylene hydride complexes with an Si*H* substituent, and exposure of $\mathbf{4^R}$ to ethylene may provide a route to silene complexes bearing an Si*H* substituent.

Herein, we report the reactions of disilyl hydride complexes $\mathbf{4^R}$ with ethylene to generate the first examples of silene complexes with a hydrogen substituent on silicon. Their unique reactivity is also described, including (a) silene hydride to silylene hydride isomerization, and (b) reaction with a second equivalent of ethylene to convert the Si*H* substituent to an Si*Et* group. The reactions of $\mathbf{4^R}$ with ethylene likely proceed *via* a low-coordinate silyl or silylene hydride intermediate, and DFT calculations, high temperature NMR spectroscopy, and trapping studies are described, providing insight into the accessibility of these intermediates.

All of the silyl, silylene and silene complexes in this work are accessed *via* reactions of [(dmpe)$_2$MnH(C$_2$H$_4$)] (**1**) with hydrosilanes, in some cases followed by ethylene. Therefore, ethylene (C$_2$H$_4$ and C$_2$D$_4$) hydrosilylation was investigated using [(dmpe)$_2$MnH(C$_2$H$_4$)] (**1**) in combination with primary and secondary hydrosilanes, and a catalytic cycle is proposed (based on the metal species and hydrosilane products observed throughout the course of the reactions). Alkene hydrosilylation is an industrially important transition metal-catalysed process for alkylsilane production,[37–39] and the most common olefin hydrosilylation catalyst used in industry is Karstedt's catalyst, [Pt$_2$(O{SiMe$_2$(CH=CH$_2$)}$_2$)$_3$].[38] However, the development of catalytic systems based on first row transition metals such as manganese is of interest due to high abundance, low cost, reduced toxicity, and improved environmental compatibility.[40] In this regard, manganese mediated hydrosilylation of polar unsaturated bonds has been well studied,[41] but only a handful of manganese catalysts have been reported for alkene hydrosilylation.[32,42]

The typical mechanism for alkene hydrosilylation (Chalk–Harrod mechanism) involves oxidative addition of a hydrosilane to generate a silyl hydride complex, followed by alkene coordination, C–H bond-forming 1,2-insertion, and finally Si–C bond-forming reductive elimination. However, in some cases alkene coordination is followed by C–Si bond-forming 1,2-insertion and then C–H bond-forming reductive elimination (modified Chalk–Harrod mechanism). Furthermore, catalytic cycles which proceed *via* a monosilyl complex rather than a silyl hydride complex have been reported, including hydrosilylation reactions utilizing a cationic palladium(II) or cobalt(III) alkyl pre-catalyst.[38,43]

Results and discussion

Reactions of disilyl hydride complexes $\mathbf{4^R}$ with ethylene

The disilyl hydride complexes [(dmpe)$_2$MnH(SiH$_2$R)$_2$] ($\mathbf{4^{Ph}}$: R = Ph, $\mathbf{4^{Bu}}$: R = ^{n}Bu) reacted with ethylene at room temperature to afford the silene hydride complexes [(dmpe)$_2$MnH(RHSi=CHMe)] ($\mathbf{6^{Ph,H}}$: R = Ph, $\mathbf{6^{Bu,H}}$: R = ^{n}Bu). This reaction mirrors the reactions of silylene hydride complexes $\mathbf{3^{R2}}$ with ethylene (*vide supra*: Scheme 1).[32] Moreover, complexes $\mathbf{6^{R,H}}$ reacted with a second equivalent of ethylene to form silene hydride complexes with two hydrocarbyl groups on Si, [(dmpe)$_2$MnH(REtSi=CHMe)] ($\mathbf{6^{Ph,Et}}$: R = Ph, $\mathbf{6^{Bu,Et}}$: R = ^{n}Bu); the products of apparent ethylene insertion into the Si–H bond (Scheme 3 and Fig. 2). This silene Si*H* to Si*R* conversion reaction is unprecedented. Complexes $\mathbf{6^{R,Et}}$ also reacted further with ethylene to generate [(dmpe)$_2$MnH(C$_2$H$_4$)] (**1**),[31] potentially by substitution of the silene ligand which undergoes subsequent decomposition to unidentified products.

A range of byproducts were observed in the syntheses of silene hydride complexes, including primary, secondary, and tertiary hydrosilanes {H$_{(3-n)}$SiEt$_n$R (n = 0, 1, 2; R = Ph, ^{n}Bu)};[45] the latter two are formed by stepwise manganese-catalysed hydrosilylation reactions between the primary hydrosilane byproduct and excess ethylene (*vide infra*). For R = ^{n}Bu, silene Si*H* to Si*Et* conversion did not proceed until all of the primary hydrosilane byproduct had been consumed, so conversion of $\mathbf{4^{Bu}}$ to $\mathbf{6^{Bu,H}}$, and then to $\mathbf{6^{Bu,Et}}$, proceeded in a stepwise fashion. By contrast, for R = Ph, silene Si*H* to Si*Et* conversion commenced as soon as $\mathbf{6^{Ph,H}}$ was available (Fig. 2).

Compounds $\mathbf{6^{Bu,H}}$ and $\mathbf{6^{Ph,Et}}$ were isolated as a red oil and a brown solid, respectively, in >95% purity. By contrast, $\mathbf{6^{Ph,H}}$ and $\mathbf{6^{Bu,Et}}$ were characterized *in situ* by NMR spectroscopy (Table 1). Compounds $\mathbf{6^{Ph,H}}$ and $\mathbf{6^{Bu,Et}}$ were not isolated due to the formation of mixtures of products (*e.g.* $\mathbf{6^{Ph,H}}$ accompanied by $\mathbf{6^{Ph,Et}}$ and **1**), combined with instability in solution over a period of days at room temperature.

In solution (in the absence of ethylene or free hydrosilanes), Si*H*-containing silene hydride complex $\mathbf{6^{Bu,H}}$ underwent isomerization to the silylene hydride complex *trans*-[(dmpe)$_2$MnH(=SiEt^{n}Bu)] (***trans*-3^{Bu,Et}**; Scheme 4), with 20% conversion after 2 days at room temperature in C$_6$D$_6$.[46] NMR spectra of ***trans*-3^{Bu,Et}** feature an Mn*H* ^{1}H NMR peak at

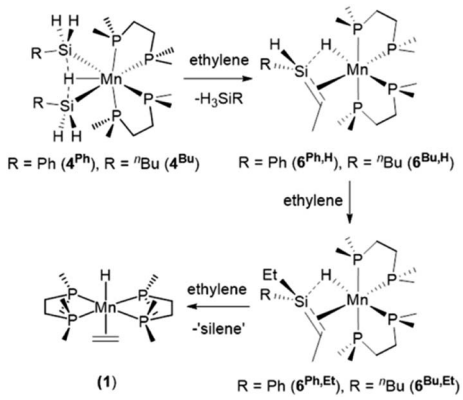

Scheme 3 Reactions of disilyl hydride complexes [(dmpe)$_2$MnH(SiH$_2$R)$_2$] ($\mathbf{4^{Ph}}$: R = Ph, $\mathbf{4^{Bu}}$: R = ^{n}Bu) with one, two, or three equivalents of ethylene to afford Si*H*-containing silene hydride complexes [(dmpe)$_2$MnH(RHSi=CHMe)] ($\mathbf{6^{Ph,H}}$: R = Ph, $\mathbf{6^{Bu,H}}$: R = ^{n}Bu), silene hydride complexes with two hydrocarbyl groups on Si [(dmpe)$_2$MnH(REtSi=CHMe)] ($\mathbf{6^{Ph,Et}}$: R = Ph, $\mathbf{6^{Bu,Et}}$: R = ^{n}Bu), and ethylene hydride complex [(dmpe)$_2$MnH(C$_2$H$_4$)] (**1**), respectively. Only one isomer is shown for each silene hydride complex.

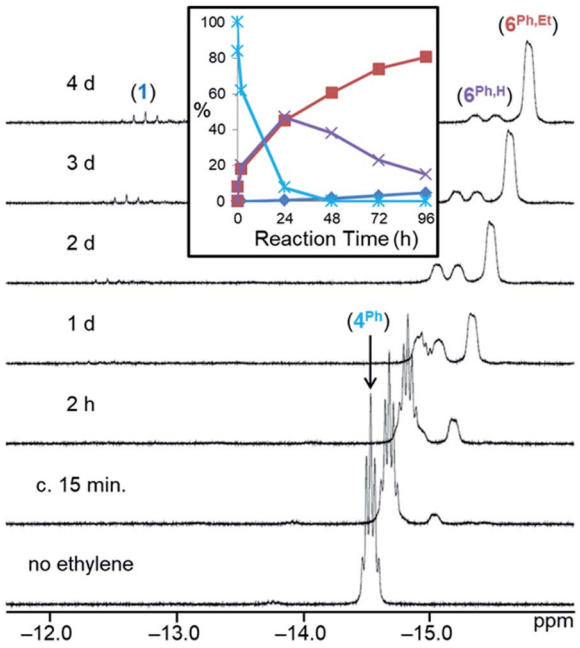

Fig. 2 ^{1}H NMR spectra (298 K, C_6D_6, 600 MHz) for the reaction of [(dmpe)$_2$MnH(SiH$_2$Ph)$_2$] ($\mathbf{4^{Ph}}$) with ethylene over time (initial, $n_{C_2H_4} \approx n_{silane}$).[44] The *x*-axis corresponds to the bottom spectrum, and for clarity, each spectrum above that is shifted by 0.15 ppm to lower frequency. The inset shows the relative concentration of hydride-containing species *versus* time; reactant [(dmpe)$_2$MnH(SiH$_2$Ph)$_2$] ($\mathbf{4^{Ph}}$; light blue ✳), silene hydride [(dmpe)$_2$MnH(PhHSi=CHMe)] ($\mathbf{6^{Ph,H}}$; purple ×), silene hydride [(dmpe)$_2$MnH(PhEtSi=CHMe)] ($\mathbf{6^{Ph,Et}}$; red ■), and [(dmpe)$_2$MnH(C_2H_4)] (**1**; dark blue ◆).

−10.48 ppm (a quintet with $^{2}J_{H,P}$ of 51 Hz), two sharp singlets in the ^{31}P{^{1}H} NMR spectrum at 80.35 and 80.50 ppm, and a high-frequency peak in the ^{29}Si{^{1}H} NMR spectrum at 364 ppm. These data are consistent with a high-symmetry base-free silylene complex, and are nearly identical to the NMR data for *trans*-[(dmpe)$_2$MnH(=SiEt$_2$)] (***trans*-$\mathbf{3^{Et2}}$**).[47] Isomerization was accompanied by formation of small amounts (~10% relative to $\mathbf{3^{Bu,Et}}$) of an unidentified

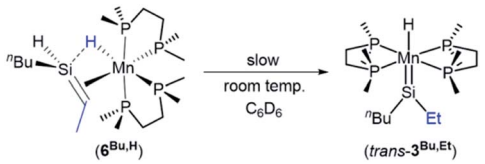

Scheme 4 Solution decomposition of [(dmpe)$_2$MnH(^{n}BuHSi=CHMe)] ($\mathbf{6^{Bu,H}}$) to form silylene complex *trans*-[(dmpe)$_2$MnH(=SiEt^{n}Bu)] (***trans*-$\mathbf{3^{Bu,Et}}$**) as the major product.

manganese hydride complex (with a quintet ^{1}H NMR peak at −9.06 ppm; $^{2}J_{H,P}$ = 47 Hz) and the silene hydride complex [(dmpe)$_2$MnH(^{n}BuEtSi=CHMe)] ($\mathbf{6^{Bu,Et}}$).

Isomerization of a silene hydride complex to a silylene hydride complex is, to our knowledge, unprecedented. However, this isomerization is related to Tilley and Bergman's report of an equilibrium between the silylene alkyl complex [Cp*(Me$_3$P)Ir(Me)(=SiMe$_2$)]$^{+}$ and the silene hydride isomer, [Cp*(Me$_3$P)IrH(Me$_2$Si=CH$_2$)]$^{+}$, which relies upon reversible α-Me and β-H elimination from a trimethylsilyl intermediate.[28]

For silene hydride complexes $\mathbf{6^{R,H}}$ (those with a hydride substituent on Si), two sets of NMR signals were observed due to a pair of isomers present in solution with a 1 : 1 ($\mathbf{6^{Ph,H}}$; Fig. 2) or 1.9 : 1 ($\mathbf{6^{Bu,H}}$) ratio, whereas only a single set of NMR signals (indicative of a single isomer) was observed for $\mathbf{6^{R,Et}}$ (silene hydride complexes with two hydrocarbyl substituents on Si). NMR spectra of the silene hydride complexes feature (for each isomer) four ^{31}P NMR signals, a single ^{29}Si NMR environment (at −17.4 to 0.7 ppm), a low frequency ^{13}C NMR signal for the Si=*C* environment (at −19.3 to −21.7 ppm), and a silene $^{1}J_{C,H}$ coupling constant (137–139 Hz) intermediate between those typical for sp^2 and sp^3 hybridized carbon atoms; Table 1. Additionally, the Mn*H* signal was located at −14.5 to −15.3 ppm in the ^{1}H NMR spectra of $\mathbf{6^{R,H}}$ and $\mathbf{6^{R,Et}}$, and the Si*H*, Si=C*H*(CH$_3$) and Si=CH(C*H*$_3$) signals were observed at 3.7 to 4.5 ppm, −0.2 to 0.2 ppm, and 1.7 to 1.9 ppm, respectively. These data are very similar to those for [(dmpe)$_2$MnH(R$_2$Si=CHMe)] ($\mathbf{6^{Ph2}}$: R = Ph, $\mathbf{6^{Et2}}$: R = Et; pertinent NMR data is included in Table 1), which have been

Table 1 Selected ^{1}H, ^{13}C, ^{29}Si and ^{31}P NMR chemical shifts (ppm) and coupling constants (Hz) for silene hydride complexes [(dmpe)$_2$MnH(RR′Si=CHMe)] ($\mathbf{6^{Ph2}}$: R = R′ = Ph; $\mathbf{6^{Et2}}$: R = R′ = Et; $\mathbf{6^{Ph,H}}$: R = Ph, R′ = H; $\mathbf{6^{Bu,H}}$: R = ^{n}Bu, R′ = H; $\mathbf{6^{Ph,Et}}$: R = Ph, R′ = Et; $\mathbf{6^{Bu,Et}}$: R = ^{n}Bu, R′ = Et); in C_6D_6 ($\mathbf{6^{R2}}$ and $\mathbf{6^{Ph,Et}}$) or d_8-toluene ($\mathbf{6^{R,H}}$ and $\mathbf{6^{Bu,Et}}$). Unless otherwise noted, values are from NMR spectra at 298 K. For $\mathbf{6^{R,H}}$, NMR environments are reported for both observed isomers. Chemical shifts for $\mathbf{6^{Ph2}}$ and $\mathbf{6^{Et2}}$ are from our prior communication[32]

	$\mathbf{6^{Ph,H}}$	$\mathbf{6^{Bu,H}}$	$\mathbf{6^{Ph,Et}}$	$\mathbf{6^{Bu,Et}}$	$\mathbf{6^{Ph2}}$	$\mathbf{6^{Et2}}$
Mn*H*	−14.5, −14.7	−14.9,[a] −15.0[b]	−14.9	−15.3	−14.6	−15.3
Si*H*	4.5[c]	3.7[c]	—	—	—	—
Si=C*H*CH$_3$	0.1, 0.2	−0.1,[a] −0.2[b]	0.2	−0.1	0.4	0.0
Si=CHC*H*$_3$	1.9[c]	1.8,[a] 1.7[b]	1.9	1.7	2.1	1.8
Si=*C*	−21.0, −21.2	−19.3,[a] −20.8[b]	−21.7	−19.3	−22.9	−19.4
^{29}Si	−7.1,[d] −17.4[d]	−8.9,[a] −17.0[b]	0.7	−6.5	−1.5	−3.0
^{31}P	63.3–85.5	65.8–79.1	65.7–79.2	65.5–79.3	62.7–78.3	65.5–79.3
$^{1}J_{C,H}$[e]	139[f]	138,[a] 139[b]	137	138	136	137

[a] Due to the minor isomer of $\mathbf{6^{Bu,H}}$. [b] Due to the major isomer of $\mathbf{6^{Bu,H}}$. [c] Both isomers have identical chemical shifts. [d] Measured at 213 K {because this environment was not located by ^{29}Si{^{1}H} or 2D ^{1}H–^{29}Si (HSQC or HMBC) NMR spectroscopy at 298 K}. [e] Coupling between the Si=*C* and Si=C*H*CH$_3$ environments. [f] $^{1}J_{C,H}$ could only be resolved for one isomer.

spectroscopically, and (for $\mathbf{6}^{\mathbf{Ph2}}$) crystallographically, characterized.[32] To the best of our knowledge, $\mathbf{6}^{\mathbf{R,H}}$ are the first spectroscopically observed[48] examples of transition metal silene complexes with a hydrogen substituent on silicon.

Despite numerous attempts, we were unable to obtain X-ray quality crystals of $\mathbf{6}^{\mathbf{R,H}}$ or $\mathbf{6}^{\mathbf{R,Et}}$. Therefore, we turned to DFT calculations in order to gain further insight into the structures of these complexes (ADF, gas-phase, all-electron, PBE, D3-BJ, TZ2P, ZORA). For all four complexes, energy minima were located for four *cis* silene hydride isomers[49] with *E* or *Z* silene stereochemistry, and differing in the orientation of the silene methyl substituent (RR′Si=CH*Me*) relative to the two dmpe ligands, as shown in Fig. 3 (see Fig. 4 for the lowest energy isomer of $\mathbf{6}^{\mathbf{Bu,H}}$). In all cases, isomers (i) and (ii) are within a few kJ mol^{-1} of one another, and are 13–22 kJ mol^{-1} lower in energy than isomers iii and iv, consistent with observation of just 2 isomers in the solution NMR spectra of $\mathbf{6}^{\mathbf{R,H}}$.[50] By contrast, the apparent formation of a single isomer of compounds $\mathbf{6}^{\mathbf{R,Et}}$ suggests that these reactions proceed under kinetic control.

In the calculated structures of silene hydride isomers (i) and (ii) (for bond metrics, see Table S4†), the Si=C bond distances of 1.80–1.81 Å fall within the range for previously reported transition metal silene complexes (1.78(2)–1.838(11) Å),[51] and correspond to Mayer bond orders ranging from 0.96 to 1.10 (*cf.* 0.70–0.91 for Si–C single bonds in the same complexes). Also, as in previously reported $\mathbf{6}^{\mathbf{R2}}$,[32] significant interligand interactions exist between silicon and the hydride. Computationally, this is illustrated by short Si–H_{Mn} distances (1.64–1.66 Å), with substantial Mayer bond orders (0.45–0.49),[52] and is also reflected by a large negative ^{29}Si–$^{1}H_{Mn}$ coupling constant of −80 Hz (measured using ^{29}Si_edited 2D ^{1}H–^{1}H COSY NMR spectroscopy)[36] for the major isomer of $\mathbf{6}^{\mathbf{Bu,H}}$ (*cf.* −30 to −31 Hz for $\mathbf{4}^{\mathbf{R}}$ and >0 in classical silyl hydride complexes).[36,53] Short Mn–Si distances (2.35–2.42 Å) with Mayer bond orders of 0.49–0.53, and Mn–H distances of 1.64–1.66 Å with Mayer bond orders of 0.52–0.56, combined with the short Si=C distance (*vide supra*), support the identification $\mathbf{6}^{\mathbf{R,H}}$ and $\mathbf{6}^{\mathbf{R,Et}}$ as *cis* silene hydride

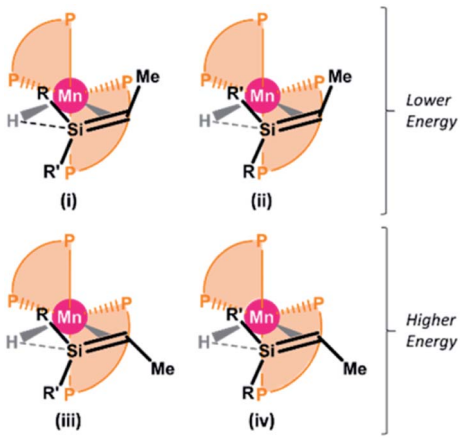

Fig. 3 Calculated isomers (i–iv) of silene hydride complexes [(dmpe)$_2$MnH(RR′Si=CHMe)] ($\mathbf{6}^{\mathbf{Ph,H}}$: R = Ph, R′ = H; $\mathbf{6}^{\mathbf{Bu,H}}$: R = ^{n}Bu, R′ = H; $\mathbf{6}^{\mathbf{Ph,Et}}$: R = Ph, R′ = Et; $\mathbf{6}^{\mathbf{Bu,Et}}$: R = ^{n}Bu, R′ = Et) featuring Si–H interligand interactions.

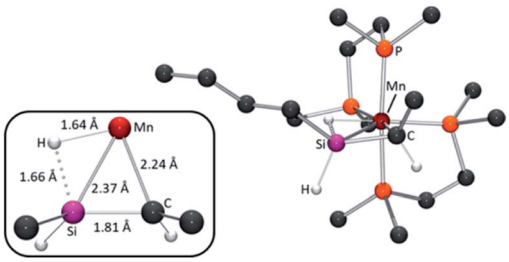

Fig. 4 Calculated structure (ball and stick diagram) for the lowest energy isomer of silene hydride complex [(dmpe)$_2$Mn(^{n}BuHSi=CHMe)] ($\mathbf{6}^{\mathbf{Bu,H}}$). All hydrogen atoms have been omitted for clarity except those on Mn or the Si=C unit. The inset shows a top-down view of the Mn silene hydride core, with selected bond distances.

complexes, as opposed to 5-coordinate alkyl complexes with a strong β-Si–H–Mn interaction.

DFT calculations on low-coordinate silyl and silylene hydride intermediates derived from $\mathbf{4}^{\mathbf{R}}$

The reactions of the disilyl hydride complexes [(dmpe)$_2$MnH(SiH$_2$R)$_2$] ($\mathbf{4}^{\mathbf{Ph}}$: R = Ph, $\mathbf{4}^{\mathbf{Bu}}$: R = ^{n}Bu) with C_2H_4 (*vide supra*) likely proceed *via* either (a) 5-coordinate mono-silyl intermediates, [(dmpe)$_2$Mn(SiH$_2$R)] ($\mathbf{2}^{\mathbf{Ph}}$: R = Ph, $\mathbf{2}^{\mathbf{Bu}}$: R = ^{n}Bu), or (b) silylene hydride intermediates, [(dmpe)$_2$MnH(=SiHR)] ($\mathbf{3}^{\mathbf{Ph,H}}$: R = Ph, $\mathbf{3}^{\mathbf{Bu,H}}$: R = ^{n}Bu), formed by sequential hydrosilane reductive elimination and α-hydride elimination from disilyl hydride complexes $\mathbf{4}^{\mathbf{R}}$ (Scheme 6; *vide infra*). Therefore, DFT calculations (ADF, gas-phase, all-electron, PBE, D3-BJ, TZ2P, ZORA) were carried out to assess the thermodynamic accessibility of such intermediates (Fig. 5 and Table 2).

In the case of low-coordinate silyl species, energy minima were located for structures in which the silyl group is either *cis* (***cis*-2$^{\mathbf{R}}$**) or *trans* (***trans*-2$^{\mathbf{R}}$**) to the vacant coordination site generated by hydrosilane reductive elimination. At 298 K, Δ*G* for the formation of these monosilyl compounds and free hydrosilane from $\mathbf{4}^{\mathbf{R}}$ is very similar (63–71 kJ mol^{-1}).

In the global minima for the *cis* isomers (rotamer 1 of ***cis*-2$^{\mathbf{R}}$**), the hydrocarbyl substituent on silicon engages in a γ-agostic interaction with manganese (*via* an *ortho*-C*H* bond in ***cis*-2$^{\mathbf{Ph}}$** or a $CH_2CH_2CH_2CH_3$ bond in ***cis*-2$^{\mathbf{Bu}}$**), with Mn–H_γ distances of 1.91–1.93 Å. The Mn–H_γ–C_γ angles in this rotamer of ***cis*-2$^{\mathbf{R}}$** are 115.9° and 131.4°, respectively, and the presence of a γ-agostic interaction is further supported by Mayer bond orders of 0.22–0.24 between Mn and H_γ, and 0.13–0.15 between Mn and C_γ.

For the phenyl analogue $\mathbf{2}^{\mathbf{Ph}}$, a higher-energy *cis* isomer was also located, corresponding to a rotamer where one of the two hydrogen substituents on silicon is now oriented in the direction of the vacant coordination site (rotamer 2 of ***cis*-2$^{\mathbf{Ph}}$**; Fig. 5 and Table 2). Relative to rotamer 1, this structure features an acute Mn–Si–H_{Si} angle of 101° (*cf.* 119°), an Mn–H_{Si} Mayer bond order of 0.06 (*cf.* <0.05), a marginally elongated Si–H_{Si} distance of 1.53 Å (*cf.* 1.51 Å), and a marginally lower Si–H_{Si} Mayer bond order of 0.80 (*cf.* 0.85), together suggestive of a weak α-Si–H–Mn interaction. Rotamer 2 of $\mathbf{2}^{\mathbf{R}}$ is presumably involved in silylene hydride formation *via* α-hydride elimination, and indeed, all

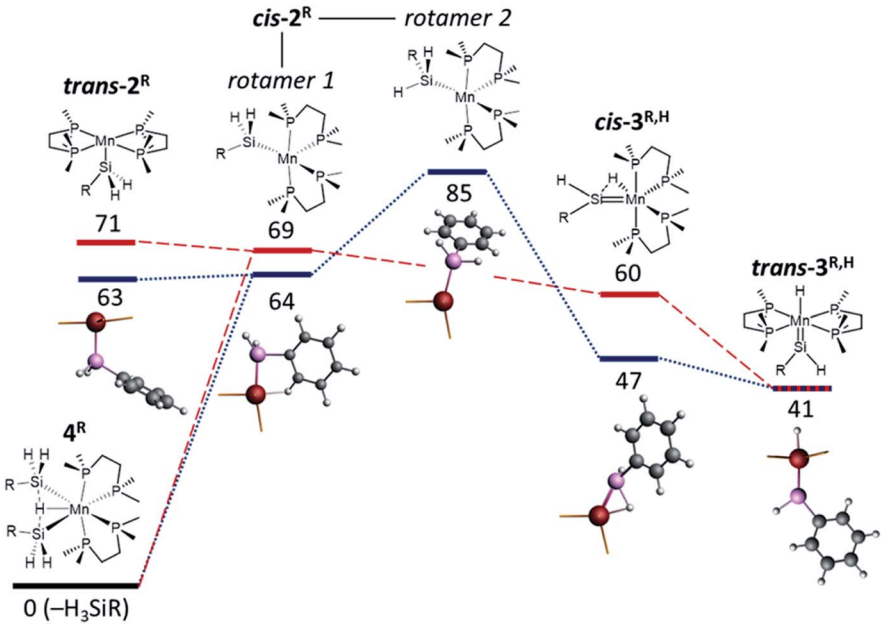

Fig. 5 DFT calculated Gibbs free energies at 298.15 K ($\Delta G^{298.15\ K}$; kJ mol^{-1}) to access reactive intermediates (and the H_3SiR byproduct) from disilyl hydride complexes [(dmpe)$_2$MnH(SiH$_2$R)$_2$] (**4^{Ph}**: R = Ph, blue dotted lines; **4^{Bu}**: R = ^{n}Bu, red dashed lines). Calculated intermediates (left to right) are: (i) an isomer of [(dmpe)$_2$Mn(SiH$_2$R)] with an equatorial dmpe arrangement (***trans*-2^{Ph}**: R = Ph, ***trans*-2^{Bu}**: R = ^{n}Bu), (ii) an isomer of [(dmpe)$_2$Mn(SiH$_2$R)] with a disphenoidal dmpe arrangement and a hydrocarbyl substituent on silicon oriented towards the vacant coordination site {rotamer 1 of ***cis*-2^{R}**: R = Ph (***cis*-2^{Ph}**), ^{n}Bu (***cis*-2^{Bu}**)}, (iii) an isomer of [(dmpe)$_2$Mn(SiH$_2$R)] with a disphenoidal dmpe arrangement and an Si*H* substituent oriented towards the vacant coordination site {rotamer 2 of ***cis*-2^{R}**: R = Ph (***cis*-2^{Ph}**); a minimum was not located for R = ^{n}Bu}, (iv) an isomer of [(dmpe)$_2$MnH(=SiHR)] with interacting *cis*-disposed silylene and hydride ligands (***cis*-3^{Ph,H}**: R = Ph, ***cis*-3^{Bu,H}**: R = ^{n}Bu), and (v) *trans*-[(dmpe)$_2$MnH(=SiHR)] (***trans*-3^{Ph,H}**: R = Ph, ***trans*-3^{Bu,H}**: R = ^{n}Bu). Geometry optimized cores of the phenyl analogues of reactive intermediates are depicted below each energy level, showing Mn in red, Si in pink, C in dark grey, and H in light grey, accompanied by stick bonds to the phosphorus donor atoms.

Table 2 Thermodynamic parameters calculated by DFT for the formation of intermediates in Fig. 5 from disilyl hydride complexes [(dmpe)$_2$MnH(SiH$_2$R)$_2$] {**4^{Ph}** (R = Ph)/**4^{Bu}** (R = ^{n}Bu)}; ΔE (calculated before ZPE correction), ΔH, $\Delta G^{298.15\ K}$, $\Delta G^{335\ K}$ (kJ mol^{-1} at 298.15 K or, for $\Delta G^{335\ K}$, 335 K), and ΔS (J mol^{-1} K^{-1} at 298.15 K)[a]

	***trans*-2^{R}**	***cis*-2^{R}** rotamer 1	***cis*-2^{R}** rotamer 2	***cis*-3^{R,H}**	***trans*-3^{R,H}**
ΔE	146/156	131/145	165/n.o.	110/115	115/122
ΔH	135/150	123/138	152/n.o.	117/124	100/111
ΔS	242/265	197/232	225/n.o.	234/216	199/234
$\Delta G^{298.15\ K}$	63/71	64/69	85/n.o.	47/60	41/41
$\Delta G^{335\ K}$	54/62	57/60	76/n.o.	39/52	34/33

[a] n.o. = not observed (*i.e.* energy minimum not located).

attempts to locate an analogous energy minimum for the ^{n}Bu analogue structure led instead to a silylene hydride structure (***cis*-3^{Bu,H}**; *vide infra*).

As with the 5-coordinate silyl species (*vide supra*), multiple energy minima (Fig. 5 and Table 2) were located for silylene hydride structures [(dmpe)$_2$MnH(=SiHR)] (**3^{Ph,H}**: R = Ph, **3^{Bu,H}**: R = ^{n}Bu). The two lowest energy structures are (a) a *cis* silylene hydride isomer with a significant interaction between silicon and the neighbouring hydride ligand (the Si$\cdots$H$_{Mn}$ distances are 1.68 Å, with Mayer bond orders of 0.52; *cf.* 0.84–0.85 for the terminal Si–H bonds), and (b) a *trans* silylene hydride isomer. These isomers are isostructural to the X-ray crystal structures of *cis*-[(dmpe)$_2$MnH(=SiPh$_2$)] (**3^{Ph2}**) and *trans*-[(dmpe)$_2$MnH(=SiEt$_2$)] (**3^{Et2}**), respectively.[32] Calculated ΔG values to access **3^{R,H}** from **4^{R}** range from 41 kJ mol^{-1} (*trans* isomers) to 47–60 kJ mol^{-1} (*cis* isomers) at 298.15 K, decreasing to 33–34 kJ mol^{-1} (*trans* isomers) and 39–52 kJ mol^{-1} (*cis* isomers) at 335 K, highlighting their thermodynamic accessibly.

In silylene hydride complexes **3^{R,H}**, Mn–Si double bond character is apparent from relatively short Mn–Si distances (2.16–2.20 Å), Mn–Si Mayer bond orders ranging from 1.17 (***cis*-3^{R,H}**) to 1.54–1.57 (***trans*-3^{R,H}**), and a planar or near-planar environment about Si ($\sum$(R–Si–R) > 356°); Table S2.† These parameters are comparable to those previously observed and/or calculated for the two isomers of [(dmpe)$_2$MnH(=SiR$_2$)] (**3^{R2}**; R = Et or Ph).[32]

High temperature NMR spectra of 4^{R}: *in situ* generation of *trans*-silylene hydride (*trans*-3^{R,H}) species

At 335 K, ^{1}H NMR spectra of the disilyl hydride complexes [(dmpe)$_2$MnH(SiH$_2$R)$_2$] (**4^{Ph}**: R = Ph, **4^{Bu}**: R = ^{n}Bu) revealed the formation of a small amount of a new manganese complex and free hydrosilane (H_3SiR; R = Ph or ^{n}Bu). This process is reversible, and clean spectra of **4^{R}** were observed upon cooling back to room temperature. The new manganese complex

exhibits a high frequency (9.83 or 9.53 ppm) and a low frequency (−9.01 or −9.60 ppm) ^{1}H NMR signal. The former is in the range observed for the terminal =SiR*H* (R = hydrocarbyl substituent) environment in diamagnetic silylene complexes of Mo, W, Fe, Ru, Os, and Ir, (6.34–12.1 ppm),[19,20,22–26] while the latter is consistent with a metal hydride environment. The low frequency hydride signal is a quintet ($^2J_{^1H,^{31}P}$ = 54 or 51 Hz) consistent with a hydride ligand apical to a plane of four equivalent phosphine donors. Taken together, these data suggest that the new complex observed at elevated temperature is *trans*-[(dmpe)$_2$MnH(=SiHR)] (***trans*-3^{Ph,H}**: R = Ph, ***trans*-3^{Bu,H}**: R = ^{n}Bu); the most thermodynamically accessible silyl or silylene species in Fig. 5.

Characterization of ***trans*-3^{R,H}** (R = Ph or ^{n}Bu) by ^{29}Si NMR spectroscopy was not successful since the new species were formed at very low concentrations (~4% and ~2% relative to **4^{Ph}** or **4^{Bu}**, respectively). However, EXSY NMR spectroscopy at 335 K indicates exchange between the two diastereotopic Si*H* protons in **4^{Ph}** or **4^{Bu}**, the free hydrosilane Si*H* peak, the high frequency *trans*-**3^{R,H}** silylene Si*H* environment, and the Mn*H* signals from both **4^R** and ***trans*-3^{R,H}** (shown in Fig. 6 for R = ^{n}Bu).[54] This is consistent with an equilibrium in which **4^R** eliminates free H_3SiR to form ***trans*-3^{R,H}** (*vide infra*).

Trapping experiments with isonitriles and N-heterocyclic carbenes

To provide experimental corroboration for the accessibility of 5-coordinate silyl [(dmpe)$_2$Mn(SiH$_2$R)] (**2^{Ph}**: R = Ph, **2^{Bu}**: R = ^{n}Bu) and silylene hydride [(dmpe)$_2$MnH(=SiHR)] (**3^{Ph,H}**: R = Ph, **3^{Bu,H}**: R = ^{n}Bu) species from **4^R**, reactions with neutral donor ligands were carried out, with a view towards coordination to manganese in **2^R** or silicon in **3^{R,H}** (Scheme 5).

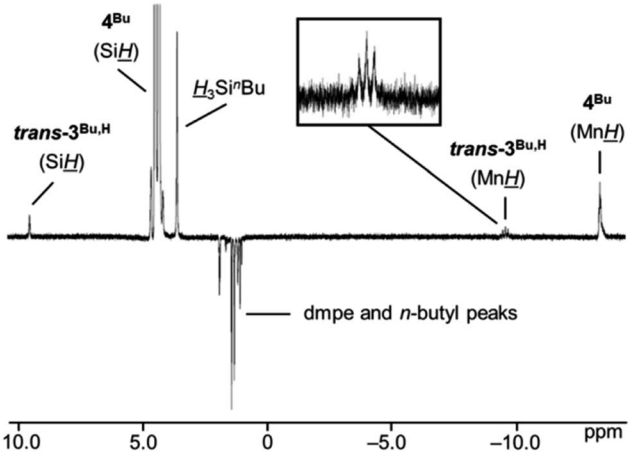

Fig. 6 1D NOESY/EXSY NMR spectrum of a solution of [(dmpe)$_2$-MnH(SiH$_2$^{n}Bu)$_2$] (**4^{Bu}**) at 335 K with excitation at the Si*H* signal of **4^{Bu}**, showing chemical exchange between the Si*H* and Mn*H* environments of [(dmpe)$_2$MnH(SiH$_2$^{n}Bu)$_2$] (**4^{Bu}**) and *trans*-[(dmpe)$_2$MnH(=SiH^{n}Bu)] (***trans*-3^{Bu,H}**), and the Si*H* environment of free H_3Si^nBu. Positive (EXSY) peaks are indicative of chemical exchange and negative (NOESY) peaks are indicative of through-space coupling (500 MHz, C_6D_6).

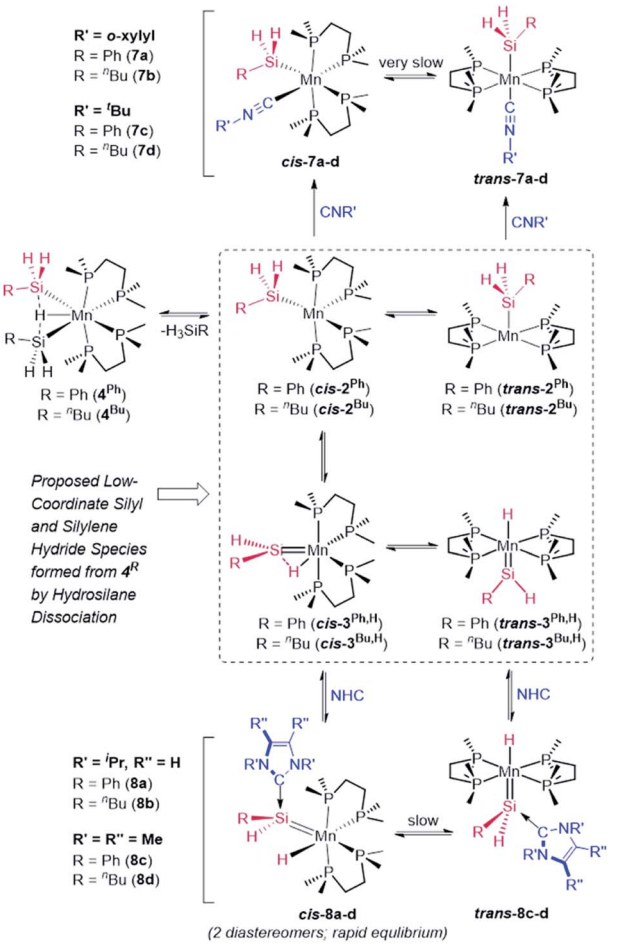

Scheme 5 Trapping of putative silyl (**2^R**) and silylene hydride (**3^{R,H}**) intermediates: synthesis of silyl isonitrile complexes [(dmpe)$_2$-Mn(SiH$_2$R)(CNR′)] (**7a**: R = Ph, R′ = *o*-xylyl; **7b**: R = ^{n}Bu, R′ = *o*-xylyl; **7c**: R = Ph, R′ = ^{t}Bu; **7d**: R = ^{n}Bu, R′ = ^{t}Bu) and NHC-stabilized silylene hydride complexes [(dmpe)$_2$MnH{=SiHR(NHC)}] (**8a**: NHC = ^{iPr}NHC, R = Ph; **8b**: NHC = ^{iPr}NHC, R = ^{n}Bu; **8c**: NHC = ^{Me}NHC, R = Ph; **8d**: NHC = ^{Me}NHC, R = ^{n}Bu).

Addition of *o*-xylylN≡C or ^{t}BuN≡C to solutions of **4^R** resulted in hydrosilane elimination, and isolation of yellow or orange silyl isonitrile complexes [(dmpe)$_2$Mn(SiH$_2$R)(CNR′)] {R′ = *o*-xylyl, R = Ph (**7a**) or ^{n}Bu (**7b**); R′ = ^{t}Bu, R = Ph (**7c**) or ^{n}Bu (**7d**)}, effectively trapping silyl complexes **2^R** (Scheme 5). In solution, all four reactions initially led to mixtures of two complexes identified by NMR spectroscopy as *cis* (85–97%) and *trans* (3–15%) isomers of **7a–d.** Slow isomerization was observed between the *cis* and *trans* isomers of **7a–d** in solution, and unexpectedly, these isomerization reactions proceeded in the direction of the *trans* isomers at elevated temperature (resulting in an increase in the proportion of *trans* isomer to 44–74% after heating solutions containing exclusively the *cis* isomer at 65–80° for 4–21 days), and in the opposite direction upon leaving the same solutions at room temperature for 3 weeks (*e.g.* leaving *cis*/*trans* mixtures of **7a,b** containing 44–48% *trans* isomer at room temperature resulted in solutions containing 99% *cis* isomer after 3 weeks).

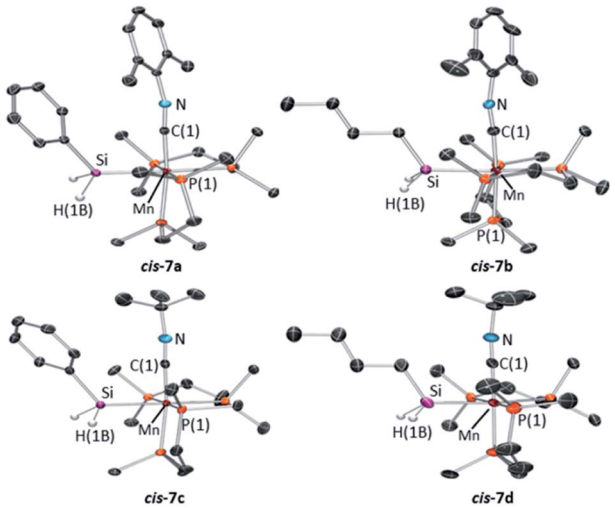

Fig. 7 X-ray crystal structures of (top left) *cis*-[(dmpe)$_2$Mn(SiH$_2$Ph)(CNxylyl)] (***cis*-7a**), (top right) *cis*-[(dmpe)$_2$Mn(SiH$_2$^{n}Bu)(CNxylyl)] (***cis*-7b**), (bottom left) *cis*-[(dmpe)$_2$Mn(SiH$_2$Ph)(CN^{t}Bu)] (***cis*-7c**), and (bottom right) *cis*-[(dmpe)$_2$Mn(SiH$_2$^{n}Bu)(CN^{t}Bu)] (***cis*-7d**), with ellipsoids drawn at 50% probability. Most hydrogen atoms have been omitted for clarity. ***cis*-7c** and ***cis*-7d** crystallized with two independent and essentially isostructural molecules in the unit cell, only one of which is shown. All structures exhibit some disorder, and only the dominant conformation is shown.

X-ray quality crystals were obtained for the four silyl isonitrile complexes **7a–d**, in each case as the *cis* isomer (Fig. 7). All four structures are octahedral with Mn–Si distances of 2.3552(5)–2.3618(5) Å and Mn–C distances of 1.805(4)–1.847(3) Å. The isonitrile ligands show elongated C$_{Mn}$–N distances of 1.176(4)–1.225(9) Å and non-linear C–N–C angles of 159.2(8)–167.5(1)°, indicative of appreciable π-backbonding.

In contrast to reactions with isonitriles, reactions of disilyl hydride complexes **4^R** with 1,3-diisopropylimidazolin-2-ylidene (^{iPr}NHC) or 1,3,4,5-tetramethyl-4-imidazolin-2-ylidene (^{Me}NHC) afforded the base-stabilized silylene hydride complexes [(dmpe)$_2$MnH{=SiHR(NHC)}] {NHC = ^{iPr}NHC, R = Ph (**8a**) or ^{n}Bu (**8b**); NHC = ^{Me}NHC, R = Ph (**8c**) or ^{n}Bu (**8d**)}, trapping the proposed silylene hydride species **3^{R,H}** (Scheme 5). Compounds **8b–d** were isolated as analytically pure red powders, whereas **8a** evaded purification.

A variety of NHC-stabilized silylene complexes have been reported for V, Cr, W, Fe, Co, Rh, and Ni,[55] and relative to base-free silylene complexes, they feature longer metal–silicon bond distances, pyramidalization at silicon, and lower frequency ^{29}Si NMR chemical shifts (typically 25–100 ppm,[56] compared with >200 ppm for base-stabilized silylene complexes).[8]

Room temperature NMR spectra of ^{iPr}NHC adducts **8a,b** revealed two sets of broad NMR signals in the process of coalescence/decalescence, due to a pair of rapidly interconverting isomers. Cooling the solutions afforded two sets of well resolved NMR signals corresponding to compounds with a disphenoidal arrangement of the phosphorus donor atoms, each with a single Si*H* signal (5.1 to 6.4 ppm), a single Mn*H* resonance (−12.3 to −12.6 ppm), a single ^{29}Si NMR environment (22.2 to 29.6 ppm), and four unique ^{31}P NMR environments (65.6–81.9 ppm). These data are indicative of NHC-coordinated *cis* silylene hydride complexes existing as a pair of interconverting diastereomers (due to chirality at Si and Mn).

In contrast, NMR spectra of the ^{Me}NHC silylene hydride complexes (**8c,d**) revealed the same two rapidly interconverting *cis* diastereomers plus a third isomer which afforded a sharp set of ^{1}H and ^{31}P NMR signals at room temperature. This third isomer corresponds to an NHC-coordinated *trans* silylene hydride complex, as evidenced by a single Mn*H* (−14.9 or −15.0 ppm) signal with a quintet coupling pattern ($^2J_{H,P}$ = 48–49 Hz) and two sharp signals in the ^{31}P{^{1}H} NMR spectra (78.7–80.6 ppm) due to diastereotopic phosphorus atoms. The ^{1}H NMR Si*H* and ^{29}Si NMR chemical shifts in these *trans* isomers (4.9–5.8 ppm and 22.4 ppm, respectively)[57] are similar to those in the *cis* isomers.

At 335 K, the two *cis* diastereomers of **8a–d** gave rise to a single set of averaged signals, with the Mn*H* peak at −12.5 to −12.7 ppm (quintets for ***cis*-8a,c,d** with $^2J_{H,P}$ = 32–34 Hz, while the NMR signal for **8b** remained a broad singlet in the process of coalescence), accompanied by (in solutions of **8c,d** only) a set of sharp signals for the *trans* isomer. For **8c,d**, EXSY NMR spectroscopy at 335 K showed cross peaks between the Mn*H* and Si*H* ^{1}H NMR signals due to both the *cis* and *trans* isomers (*i.e.* chemical exchange between all *four* environments). This equilibrium between *cis*- and *trans*-**8c,d** mirrors that previously reported between the *cis* and *trans* isomers of base-free [(dmpe)$_2$MnH(=SiPh$_2$)] (**3^{Ph2}**).[32]

Possible mechanisms for ambient temperature exchange between the *cis* diastereomers of **8a–d** are (a) phosphine donor dissociation, isomerization of the 5-coordinate product, and phosphine re-coordination, or (b) NHC dissociation to generate *cis*-[(dmpe)$_2$MnH(=SiHR)] (***cis*-3^{Ph,H}**: R = Ph, ***cis*-3^{Bu,H}**: R = ^{n}Bu), followed by re-coordination to the opposite face of the silylene ligand.[58] The latter mechanism would imply that **8a–d**, like disilyl hydride complexes **4^R**, could react as sources of either base-free silylene hydride complexes **3^{R,H}**, or 5-coordinate silyl complexes **2^R**. The accessibility of this pathway is implied by the reactions of **8d** with ^{t}BuNC, and **8b** with ethylene, which afforded [(dmpe)$_2$Mn(SiH$_2$^{n}Bu)(CN^{t}Bu)] (**7d**) and [(dmpe)$_2$MnH(^{n}BuHSi=CHMe)] (**6^{Bu,H}**),[59] respectively; these are the same complexes formed in reactions of these reagents with **4^{Bu}**. Furthermore, the accessibility of **2^R** provides a mechanism for the observed exchange between the Si*H* and Mn*H* environments in the EXSY NMR spectra of **8c,d** at 335 K (*vide supra*).

X-ray quality crystals were obtained for complexes **8a–d** by recrystallization from concentrated hexanes solutions (**8a,b**), toluene layered with pentane (**8c**), or a dilute hexanes solution (**8d**) at −30 °C. The solid state structures of **8a–c** (Fig. 8; top row and bottom left) feature a *cis* arrangement of the hydride and base-stabilized silylene ligands, corresponding to one of the two *cis* diastereomers observed in solution.[60] By contrast, **8d** crystallized as the *trans* isomer (Fig. 8; bottom right). In all four structures {complementary DFT calculations modelled **8b,d** with an ^{n}Bu group in place of the Et group; [(dmpe)$_2$MnH{=SiHEt(NHC)}] where NHC = ^{iPr}NHC (**8b***) or ^{Me}NHC (**8d***)},

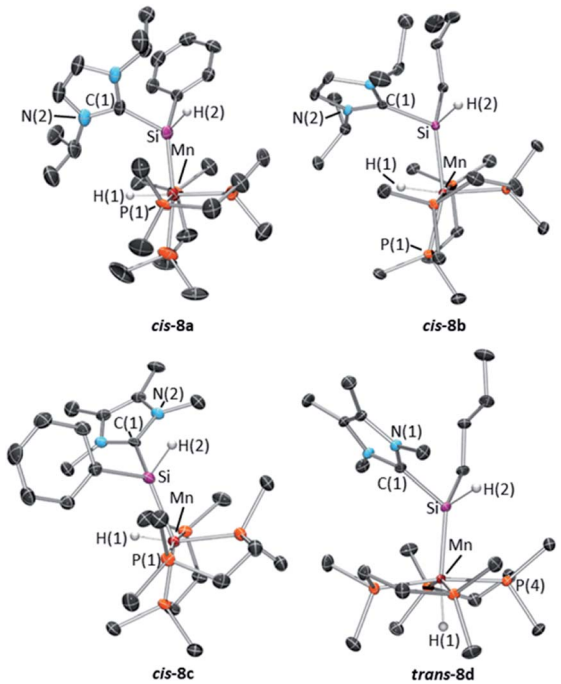

Fig. 8 X-ray crystal structures of (top left) *cis*-[(dmpe)$_2$MnH{=SiH-Ph(^{iPr}NHC)}] (***cis*-8a**), (top right) *cis*-[(dmpe)$_2$MnH{=SiH^{n}Bu(^{iPr}NHC)}] (***cis*-8b**), (bottom left) *cis*-[(dmpe)$_2$MnH{=SiHPh(^{Me}NHC)}] (***cis*-8c**), and (bottom right) *trans*-[(dmpe)$_2$MnH{=SiH^{n}Bu(^{Me}NHC)}] (***trans*-8d**) with ellipsoids drawn at 50% probability. Most hydrogen atoms have been omitted for clarity. In the case of **8a–b**, the structures exhibit some disorder, and only the dominant conformation is shown.

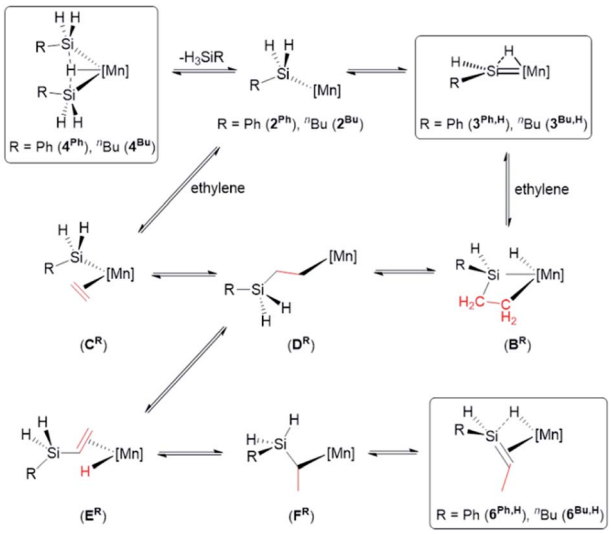

Scheme 6 Proposed pathways for reactions of disilyl hydride complexes [(dmpe)$_2$MnH(SiH$_2$R)$_2$] (**4^{Ph}**: R = Ph, **4^{Bu}**: R = ^{n}Bu) with ethylene to form silene hydride complexes [(dmpe)$_2$MnH(RHSi=CHMe)] (**6^{Ph,H}**: R = Ph, **6^{Bu,H}**: R = ^{n}Bu). [Mn] = Mn(dmpe)$_2$. Only one isomer of **3^{R,H}** is shown. Boxes indicate complexes which have been isolated or spectroscopically observed.

NHC coordination to silicon resulted in elongated Mn–Si distances (2.255(1)–2.299(1) Å; calcd 2.26–2.30 Å for both isomers of **8a,b*,c,d***), and correspondingly weaker Mayer bond orders of 1.03–1.08 (Table S6†), relative to base-free silylene complexes **3^{R,H}** (2.16–2.20 Å and 1.17–1.57, respectively). Unlike base-free analogues (*vide supra*), ***cis*-8a–d** display only negligible interligand Si–H interactions (with Mayer bond orders ≤0.13). Additionally, substantial pyramidalization at silicon was observed for both isomers of **8a–d**, where the sum of the angles around silicon (for non-NHC substituents) ranged from 322(3) to 342(2)° (calcd 336.1–341.5°; Table S6,† *cf.* >356° in **3^{R,H}**). Nevertheless, the Mn–Si distances are significantly shorter than those in related silyl complexes **7a–d** (the Mn–Si distances in **7a–d** range from 2.3552(5)–2.3618(5) Å {calcd 2.35–2.36 Å (*cis*) and 2.41–2.42 Å (*trans*), with Mayer bond orders of 0.89–0.93}),[61] indicative of residual Mn–Si multiple bond character in **8a–d**.

Pathways for reactions of 4^R with ethylene

Previously, we reported the reactions of the silylene hydride complexes, [(dmpe)$_2$MnH(=SiR$_2$)] (**3^{Ph2}**: R = Ph, **3^{Et2}**: R = Et), with ethylene to form the silene hydride complexes [(dmpe)$_2$-MnH(R$_2$Si=CHMe)] (**6^{Ph2}**: R = Ph, **6^{Et2}**: R = Et).[32] Given that disilyl hydride complexes **4^R** exist in equilibrium with analogous low-coordinate silyl and silylene hydride complexes (*vide supra*), it is likely that the reactions of **4^R** with ethylene proceed *via* a parallel mechanism, as illustrated in Scheme 6. The initial steps in this scheme involve either (a) ethylene coordination to a silylene hydride intermediate (**3^{R,H}**) followed by 2 + 2 cycloaddition (to form **B^R**) and subsequent Si–H bond-forming reductive elimination, or (b) coordination of ethylene to a low coordinate silyl intermediate (**2^R**), forming **C^R**, followed by 1,2-insertion. Both of these pathways generate primary alkyl complex **D^R**, which can provide access to **6^{R,H}** by sequential β-hydride elimination (to form **E^R**), 1,2-insertion to generate secondary alkyl complex **F^R**, and a second β-hydride elimination involving the hydrogen substituent on silicon. Consistent with this mechanism, the reactions of [(dmpe)$_2$MnH(SiH$_2$^{n}Bu)$_2$] (**4^{Bu}**) or [(dmpe)$_2$Mn{=SiH^{n}Bu(^{iPr}NHC)}] (**8b**) with d_4-ethylene yielded [(dmpe)$_2$MnH(^{n}BuHSi=CDCD$_3$)] as the only observed isotopomer of **6^{Bu,H}**.

After conversion of **4^R** to **6^{R,H}**, reaction with a second equivalent of ethylene resulted in conversion of a silene Si*H* group in **6^{R,H}** to an Si*Et* group, yielding **6^{R,Et}** (*vide supra*). This reactivity likely involves the experimentally observed isomerization of **6^{R,H}** to silylenes **3^{R,Et}** (*vide supra*), presumably *via* a low-coordinate silyl intermediate (**2^{R,Et}** in Scheme 7) formed from **6^{R,H}** by C–H bond-forming 1,2-insertion. Conversion to **6^{R,Et}** can then take place *via* previously discussed pathways (Scheme 6) involving reactions of the silylene or low-coordinate silyl species with ethylene to afford intermediates **B^{R,Et}** and **C^{R,Et}**, respectively (**B^{R,Et}** and **C^{R,Et}** are analogues of **B^R** and **C^R** in Scheme 6, but with an ethyl group in place of one hydrogen atom on silicon).[62]

Deuterium labelling studies were employed to provide experimental support for these mechanistic proposals. Specifically, [(dmpe)$_2$MnH(^{n}BuHSi=CDCD$_3$)] (**d_4_6^{Bu,H}**) isomerized to exclusively form *trans*-[(dmpe)$_2$MnH{=Si^{n}Bu(CHDCD$_3$)}] (***trans***-

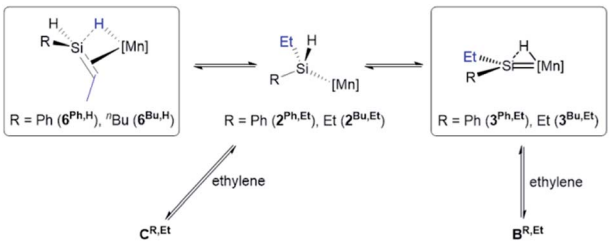

Scheme 7 Initial steps in the pathway proposed for reactions of silene hydride complexes [(dmpe)$_2$MnH(RHSi=CHMe)] ($\mathbf{6^{Ph,H}}$; R = Ph, $\mathbf{6^{Bu,H}}$: R = ^{n}Bu) with ethylene to afford [(dmpe)$_2$MnH(REtSi=CHMe)] ($\mathbf{6^{Ph,Et}}$; R = Ph, $\mathbf{6^{Bu,Et}}$: R = ^{n}Bu). [Mn] = Mn(dmpe)$_2$. Intermediates $\mathbf{B^{R,Et}}$ and $\mathbf{C^{R,Et}}$ are analogous to intermediates $\mathbf{B^R}$ and $\mathbf{C^R}$ in Scheme 6, but with an ethyl group in place of one hydrogen atom on silicon. Only one isomer of **3** is shown. Boxes indicate complexes which have been isolated or spectroscopically observed.

d*$_4$_$\mathbf{3^{Bu,Et}}$**), and the reaction of [(dmpe)$_2$MnH(^{n}BuHSi=CHMe)] ($\mathbf{6^{Bu,H}}$) with d_4-ethylene yielded [(dmpe)$_2$MnH(^{n}BuEtSi=CDCD$_3$)] (d*$_4$_$\mathbf{6^{Bu,Et}}$**). Additionally, we have previously reported that [(dmpe)$_2$MnH(=SiEt$_2$)] ($\mathbf{3^{Et2}}$) exclusively forms [(dmpe)$_2$MnH(Et$_2$Si=CDCD$_3$)] (***d*$_4$_$\mathbf{6^{Et2}}$**) upon exposure to d_4-ethylene.

Catalytic ethylene hydrosilylation

Our group previously reported that [(dmpe)$_2$MnH(Et$_2$Si=CHMe)] ($\mathbf{6^{Et2}}$) catalyses ethylene hydrosilylation by diethylsilane.[32] Upon monitoring the progress of this reaction by NMR spectroscopy, the silyl dihydride complex, [(dmpe)$_2$MnH$_2$(SiHEt$_2$)] ($\mathbf{5^{Et2}}$), silylene hydride complex [(dmpe)$_2$MnH(=SiEt$_2$)] ($\mathbf{3^{Et2}}$),[63] and ethylene hydride complex [(dmpe)$_2$MnH(C$_2$H$_4$)] (**1**), were all observed in solution, in addition to silene hydride complex $\mathbf{6^{Et2}}$. We were therefore motivated to investigate [(dmpe)$_2$MnH(C$_2$H$_4$)] (**1**) as a pre-catalyst for ethylene hydrosilylation (using primary and secondary hydrosilanes), given that it is a precursor to disilyl hydride, silylene hydride and silene hydride complexes in the presence of hydrosilanes and/or ethylene.

At 60 °C, addition of 7 mol% of [(dmpe)$_2$MnH(C$_2$H$_4$)] (**1**) to primary or secondary hydrosilanes (H$_3$SiPh, H$_3$Si^{n}Bu, H$_2$SiPh$_2$ or H$_2$SiEt$_2$) in C$_6$D$_6$ under ethylene (1.7 atm initial pressure) led to catalytic incorporation of one or two equivalents of ethylene into the Si–H bonds of the free hydrosilanes, leading to a mixture of new hydrosilanes (Table 3). The major products in reactions of secondary hydrosilanes were tertiary hydrosilanes (HSiEtPh$_2$ or HSiEt$_3$), while reactions involving primary hydrosilanes first formed secondary hydrosilanes (H$_2$SiEt^{n}Bu or H$_2$SiEtPh), followed by reaction with an additional equivalent of ethylene to generate the tertiary hydrosilane (HSiEt$_2$Ph or HSiEt$_2$^{n}Bu) as the major product. Hydrosilylation reactions with H$_3$Si^{n}Bu, H$_2$SiPh$_2$, and H$_2$SiEt$_2$ produced fewer byproducts than those with H$_3$SiPh (as noted in Table 3). Additionally, hydrosilylation with H$_2$SiEt$_2$ progressed much more rapidly than that with H$_2$SiPh$_2$. By contrast, no reactivity was observed when **1** was exposed to ethylene and the tertiary hydrosilanes HSiEt$_3$ or HSiEtPh$_2$; various other hydrosilylation catalysts exhibit higher activities than **1**, especially precious metal catalysts,[38,64] but the ability of **1** to selectively form tertiary but not quaternary hydrosilanes from ethylene is uncommon.[65]

Organic byproducts were observed during conversion of secondary to tertiary silanes, but not conversion of primary to secondary silanes. The major byproduct was a hydrosilane with a vinyl group (Vi) in place of an ethyl substituent (HSiEtViR, R = Et or ^{n}Bu or HSiPhViR, R = Et or Ph), accompanied by one or more unidentified Si*H*-containing silanes (Table 3). Vinyl silanes are commonly observed byproducts in olefin (*e.g.* H$_2$C=CHR) hydrosilylation, formed by β-hydride elimination from an M(CH$_2$CHRSiR$_3$) intermediate in the catalytic cycle,[66] and were an impetus for the initial proposal of a modified Chalk–Harrod catalytic cycle involving C–Si rather than C–H bond-forming 1,2-insertion from an alkene-coordinated silyl hydride intermediate.[37]

During catalysis using primary and secondary hydrosilanes, a variety of manganese-containing complexes were observed by NMR spectroscopy, including disilyl hydride complexes (for reactions involving primarily hydrosilanes only), silylene hydride complexes (for reactions involving secondary silanes only),[63] silyl dihydride complexes, silene hydride complexes, and ethylene hydride complex **1**. Furthermore, all of these classes of complex are catalytically active. For example, [(dmpe)$_2$MnH(Et$_2$Si=CHMe)] ($\mathbf{6^{Et2}}$)[32] and [(dmpe)$_2$MnH(=SiEt$_2$)] ($\mathbf{3^{Et2}}$) are catalysts for ethylene hydrosilylation using secondary hydrosilanes, and [(dmpe)$_2$MnH(SiH$_2$^{n}Bu)$_2$] ($\mathbf{4^{Bu}}$) and [(dmpe)$_2$MnH$_2$(SiH$_2$^{n}Bu)] ($\mathbf{5^{Bu}}$) are active for ethylene hydrosilylation by H$_3$Si^{n}Bu. Reactions involving $\mathbf{6^{Et2}}$, $\mathbf{3^{Et2}}$, and $\mathbf{4^{Bu}}$ rapidly generated distributions of Mn-containing species and hydrosilane products which are very similar to those formed when [(dmpe)$_2$MnH(C$_2$H$_4$)] (**1**) was used as the pre-catalyst. By contrast, when $\mathbf{5^{Bu}}$ was

Table 3 Ratio of hydrosilane products (assigning the tertiary hydrosilane product a value of 100) observed by ^{1}H NMR spectroscopy after hydrosilylation of ethylene catalysed by [(dmpe)$_2$MnH(C$_2$H$_4$)] (**1**) pre-catalyst (7 mol%) with 1.7 atm ethylene (initially $n_{silane} \approx n_{ethylene}$; for reactions with H$_3$SiR, the headspace was re-filled with ethylene after 1 week) at 60 °C in C$_6$D$_6$ after 50 days (H$_3$SiPh), 25 days (H$_3$Si^{n}Bu) or 6 days (H$_2$SiR$_2$)

Substrate	R/R′	Substrate	H$_2$SiEtR	HSiEtRR′	HSiViRR′	Unidentified[a]
H$_3$SiPh	Ph/Et	0	0	100	<5	20[b]
H$_3$Si^{n}Bu	^{n}Bu/Et	0	<5	100	20	10[c]
H$_2$SiPh$_2$	Ph/Ph	50	n.a.	100	<5	20
H$_2$SiEt$_2$	Et/Et	6	n.a.	100	11	<5

[a] Relative amounts of unidentified Si*H*-containing silanes were determined assuming that they contain a single Si*H* proton. [b] At least seven unassigned Si*H* environments were observed. [c] Two unassigned Si*H* environments were observed.

employed, hydrosilylation proceeded at a slower rate, and even after 24 hours the dominant manganese-containing species was $\mathbf{5^{Bu}}$.

In order to monitor ethylene hydrosilylation reactions under conditions where ethylene concentration does not vary significantly during the course of the reaction, multiple aliquots from a stock solution of **1** and H_3Si^nBu in C_6D_6 were placed under a large excess of ethylene in a sealed 50 mL flask (initial pressure 1.7 atm, $n_{C_2H_4} \approx 40 \times n_{silane}$) and heated at 60 °C for various time periods prior to analysis by NMR spectroscopy (Fig. 9). Key observations were; (a) nearly complete conversion of the primary hydrosilane to secondary hydrosilane H_2SiEt^nBu was observed *before* any formation of the tertiary silane ($HSiEt_2{}^nBu$) product or vinyl silane ($HSiEtVi^nBu$) byproduct, (b) during hydrosilylation by the primary hydrosilane H_3Si^nBu, the dominant metal-containing species was the Si*H*-containing silene hydride [(dmpe)$_2$MnH(^{n}BuHSi=CHMe)] ($\mathbf{6^{Bu,H}}$), with small amounts of the disilyl hydride [(dmpe)$_2$MnH($SiH_2{}^nBu)_2$] ($\mathbf{4^{Bu}}$), (c) after 13 hours, almost all H_3Si^nBu had been consumed, (d) from 13 to 18 hours, conversion of H_2SiEt^nBu to $HSiEt_2{}^nBu$ proceeded rapidly with concurrent formation of the vinylsilane byproduct $HSiEtVi^nBu$ (see below for experiments to determine the manganese species present *between* 13 and 18 hours), (e) after 18 hours, **1** was the dominant manganese species in solution {accompanied by small amounts of the silene hydride [(dmpe)$_2$MnH(^{n}BuEtSi=CEtMe)] ($\mathbf{6^{Bu,Et}}$) and the silyl dihydride [(dmpe)$_2$MnH$_2$(SiHEt^{n}Bu)] ($\mathbf{5^{Bu,Et}}$)}, and conversion of H_2SiEt^nBu to $HSiEt_2{}^nBu$ now proceeded more slowly, and (f) after 12 days, >99.5% of the H_2SiEt^nBu intermediate had been consumed yielding 81% $HSiEt_2{}^nBu$, 16% $HSiEtVi^nBu$, and 3% of an unidentified Si*H*-containing byproduct (assuming that this species contains one Si*H* proton), which is non-volatile at room temperature (5 mTorr); at this point, the only Mn-containing species in the reaction mixture was [(dmpe)$_2$MnH(C_2H_4)] (**1**). Relative amounts of the different hydrosilane and Mn*H*-containing species in solution during ethylene hydrosilylation by H_3Si^nBu are plotted as a function of time in Fig. 9.

Between 13 and 18 hours in Fig. 9, conversion of H_2SiEt^nBu to $HSiEt_2{}^nBu$ proceeded rapidly (to more than 50% conversion), and then slowed down dramatically, as the resting state of the catalyst switched to [(dmpe)$_2$MnH(C_2H_4)] (**1**). However, during secondary to tertiary hydrosilane conversion, [(dmpe)$_2$MnH(^{n}BuHSi=CHMe)] ($\mathbf{6^{Bu,H}}$) cannot be regenerated, indicating that a different manganese species may have spiked in concentration *between* the 13 and 18 hour data points (this species is presumably responsible for continued rapid H_2SiEt^nBu to $HSiEt_2{}^nBu$ conversion observed during this time period). Consequently, the reaction in Fig. 9 was repeated and stopped after most but not all of the primary hydrosilane had been consumed {the resulting mixture of hydrosilanes and Mn-containing species in C_6D_6 was similar to that observed at 13 h in Fig. 9; *i.e.* mostly secondary hydrosilane H_2SiEt^nBu and [(dmpe)$_2$MnH(^{n}BuHSi=CHMe)] ($\mathbf{6^{Bu,H}}$), with a small amount of the primary hydrosilane, H_3Si^nBu}. This mixture was then sealed under a near-stoichiometric (relative to the hydrosilane)

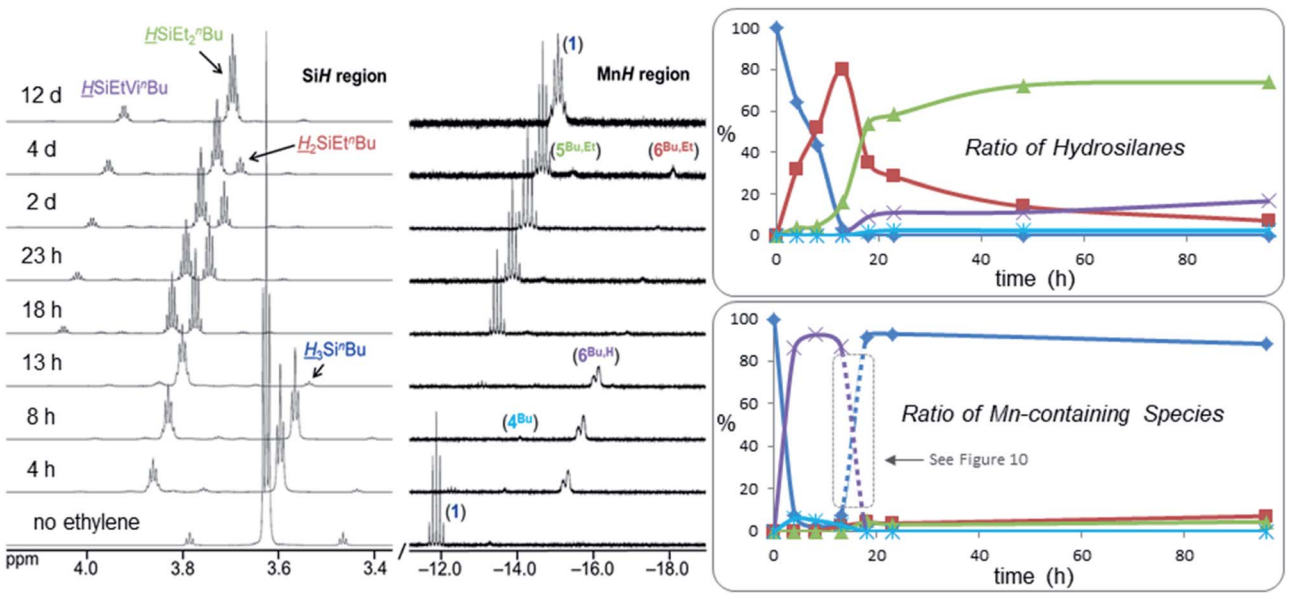

Fig. 9 Si*H* (left) and Mn*H* (middle) regions of the ^{1}H NMR spectra (298 K, 500 or 600 MHz) for the hydrosilylation of ethylene by H_3Si^nBu using [(dmpe)$_2$MnH(C_2H_4)] (**1**) pre-catalyst (7 mol% relative to the hydrosilane) under ~1.7 atm of ethylene (initial, $n_{C_2H_4} \approx 40 \times n_{silane}$) in C_6D_6 and after various time intervals at 60 °C. The *x*-axis corresponds to the bottom ^{1}H NMR spectrum, and for clarity, each spectrum above that is shifted by 0.3 (Si*H* region) or 0.4 (Mn*H* region) ppm to lower frequency. Right: graphs showing the ratio of (top) hydrosilanes (dark blue ◆ = H_3Si^nBu; red ■ = H_2SiEt^nBu; green ▲ = $HSiEt_2{}^nBu$; purple × = $HSiViEt^nBu$; light blue ✳ = unidentified Si*H*-containing silane) and (bottom) Mn*H*-containing species {dark blue ◆ = [(dmpe)$_2$MnH(C_2H_4)] (**1**); light blue ✳ = [(dmpe)$_2$MnH($SiH_2{}^nBu)_2$] ($\mathbf{4^{Bu}}$); green ▲ = [(dmpe)$_2$MnH$_2$(SiHEt^{n}Bu)] ($\mathbf{5^{Bu,Et}}$); purple × = [(dmpe)$_2$MnH(^{n}BuHSi=CHMe)] ($\mathbf{6^{Bu,H}}$); red ■ = [(dmpe)$_2$MnH(^{n}BuEtSi=CHMe)] ($\mathbf{6^{Bu,Et}}$)} in these reactions, as measured by ^{1}H NMR spectroscopy. Reaction details can be found in the ESI pg. S15.†

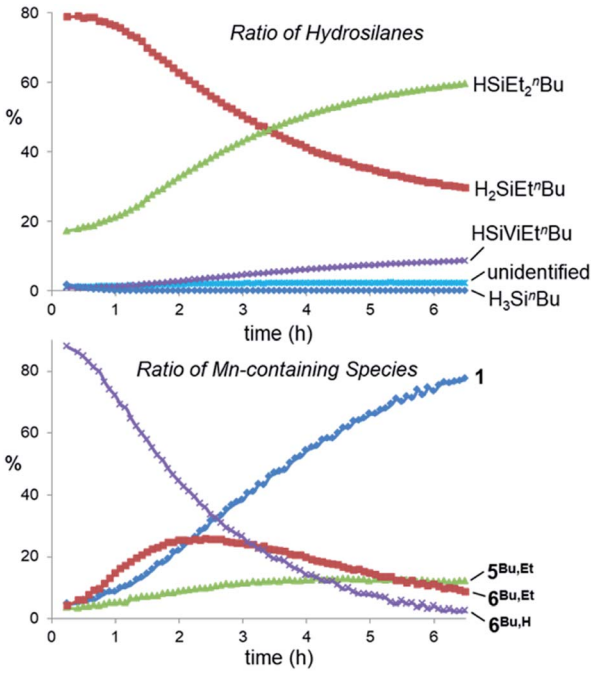

Fig. 10 Graphs showing the ratio of (top) hydrosilanes (dark blue ◆ = H_3Si^nBu; red ■ = H_2SiEt^nBu; green ▲ = $HSiEt_2{}^nBu$; purple × = $HSiViEt^nBu$; light blue ✳ = unidentified Si*H*-containing silane) and (bottom) Mn*H*-containing species {dark blue ◆ = $[(dmpe)_2MnH(C_2H_4)]$ (**1**); red ■ = $[(dmpe)_2MnH(^n BuEtSi{=}CHMe)]$ ($\mathbf{6^{Bu,Et}}$); green ▲ = $[(dmpe)_2MnH_2(SiHEt^nBu)]$ ($\mathbf{5^{Bu,Et}}$); purple × = $[(dmpe)_2MnH(^n BuEtSi{=}CHMe)]$ ($\mathbf{6^{Bu,Et}}$)} measured over time by ^{1}H NMR spectroscopy (in C_6D_6 at 56 °C) for the hydrosilylation of ethylene (initial, $n_{C_2H_4} \approx n_{silane}$) by a mixture of hydrosilanes corresponding to the 13 h mark in Fig. 9. Reaction details can be found in the ESI pg. S15.†

amount of ethylene in an NMR tube, and monitored by NMR spectroscopy at 56 °C in 5 minute intervals (Fig. 10).

In Fig. 10, consumption of remaining primary hydrosilane was complete after 10 minutes, followed by rapid secondary to tertiary hydrosilane conversion and a spike in the concentration of a new silene hydride complex, $[(dmpe)_2MnH(^n BuEtSi{=}CHMe)]$ ($\mathbf{6^{Bu,Et}}$), while the concentrations of $\mathbf{6^{Bu,H}}$ (the resting state of the catalyst during primary to secondary hydrosilane conversion) and $[(dmpe)_2MnH(C_2H_4)]$ (**1**) (the Mn-containing species dominant after the 18 h mark) diminished and increased, respectively. Furthermore, a small amount (~12%) of the silyl dihydride complex $[(dmpe)_2MnH_2(SiHEt^nBu)]$ ($\mathbf{5^{Bu,Et}}$) grew in over this time period, and vinylsilane ($HSiViEt^nBu$) production was observed to accompany the formation of **1** and $\mathbf{5^{Bu,Et}}$. The slowdown in the rate of catalysis between 13 and 18 hours in Fig. 9 can therefore be attributed to a change in the resting state of the catalyst, from more active silene hydride complexes $\mathbf{6^{Bu,H}}$ and $\mathbf{6^{Bu,Et}}$, to **1** and $\mathbf{5^{Bu,Et}}$, both of which are formed *via* vinylsilane elimination (*vide infra*), and re-enter the catalytic cycle slowly ($\mathbf{5^{Bu,Et}}$ is particularly slow to enter the cycle; *vide supra*).

A catalytic cycle (Scheme 8) can be envisaged based on the reaction pathways already proposed for (a) reaction of ethylene with disilyl hydride complexes $\mathbf{4^R}$ (formed in reactions of **1** with primary hydrosilanes) to afford silene hydride complexes $\mathbf{6^{R,H}}$, and (b) reaction of ethylene with silylene hydride complexes $\mathbf{3^{R2}}$ (formed in reactions of **1** with secondary hydrosilanes)[32] to afford silene hydride complexes $\mathbf{6^{R2}}$. These reactions are identified with blue reaction arrows in Scheme 8. In the presence of free hydrosilane substrate, the catalytic cycle can be completed (green reaction arrows) by reaction of hydrosilanes with primary alkyl intermediate **D** (pathway 'a' in Scheme 8) or secondary alkyl intermediate **F** (pathway 'b' in Scheme 8); *via* oxidative addition followed by reductive elimination, or σ-bond metathesis.[67]

Alternatively, for conversion of primary to secondary hydrosilanes, the catalytic cycle in Scheme 8 can be completed by C–H bond-forming 1,2-insertion from intermediate $\mathbf{6^{R,H}}$ (pathway 'c', green reaction arrow) to generate silyl and silylene hydride species $\mathbf{2^{R,Et}}$ and $\mathbf{3^{R,Et}}$. Isomerization of $\mathbf{6^{Bu,H}}$ to $\mathbf{3^{Bu,Et}}$ has been observed in the absence of ethylene and hydrosilanes (Scheme 4), and this pathway is also thought to be involved in the reactions of $[(dmpe)_2MnH(RHSi{=}CHMe)]$ ($\mathbf{6^{R,H}}$) with ethylene to afford $[(dmpe)_2MnH(REtSi{=}CHMe)]$ ($\mathbf{6^{R,Et}}$) in which an Si*H* group is converted to an Si*Et* group (Scheme 7). If pathway 'c' is involved in the catalysis, the resulting [Mn]SiHREt ($\mathbf{2^{R,Et}}$) complex must react with free H_3SiR to form [Mn]SiH_2R ($\mathbf{2^R}$) and eliminate H_2SiREt (likely *via* an unobserved disilyl hydride intermediate analogous to $\mathbf{4^R}$), given that the observed reactivity converts primary hydrosilanes to *free* secondary hydrosilanes prior to the formation of significant amounts of tertiary hydrosilane products. The accessibility of this reaction pathway is highlighted by the reaction of $[(dmpe)_2MnH(=SiR_2)]$ {R = Ph ($\mathbf{3^{Ph2}}$) or Et ($\mathbf{3^{Et2}}$)} with excess H_3Si^nBu at 20 °C to afford $[(dmpe)_2MnH(SiH_2{}^nBu)_2]$ ($\mathbf{4^R}$) and free H_2SiPh_2 or H_2SiEt_2, respectively. This reaction was complete in several hours (for $\mathbf{3^{Et2}}$) or minutes (for $\mathbf{3^{Ph2}}$).

Unidentified Si*H*-containing byproducts {formed in larger amounts in reactions with H_2SiPh_2 and H_3SiPh (after conversion to $H_2SiEtPh$); Table 3} may arise from reactions of **D** (or less likely **F**) with hydrosilanes resulting in C–Si rather than C–H bond-formation to eliminate a disilylated organic product and generate manganese hydride intermediate $[(dmpe)_2MnH]$ (**A**), which can re-enter the proposed catalytic cycle (*vide infra*) as shown in Scheme 8. This reactivity bears resemblance to that of '$(dmpe)_2MnEt$' (an isomer of **1**)[35] with H_2SiPh_2 to afford a 1 : 1 mixture of (a) $[(dmpe)_2MnH(=SiPh_2)]$ ($\mathbf{3^{Ph2}}$) and ethane, the products of *C–H* bond-forming oxidative addition/reductive elimination (or σ-bond metathesis) followed by α-hydride elimination, and (b) $[(dmpe)_2MnH_2(SiHPh_2)]$ ($\mathbf{5^{Ph2}}$) and Ph_2SiEtH, the products of *C–Si* bond-forming oxidative addition/reductive elimination (or σ-bond metathesis) to form $[(dmpe)_2MnH]$ (**A**), followed by oxidative addition of a second equivalent of H_2SiPh_2.[32]

Pathways 'a', 'b' and 'c' described above (green reaction arrows in Scheme 8) generate the observed disilyl hydride ($\mathbf{4^R}$), silylene hydride (**3**) and silene hydride (**6**) complexes. However, they do not explain the formation of vinyl silane byproducts. These byproducts can be accessed by vinylsilane dissociation from intermediate **E**,[68] forming low-coordinate hydride species **A**, which can react with either of the available organic

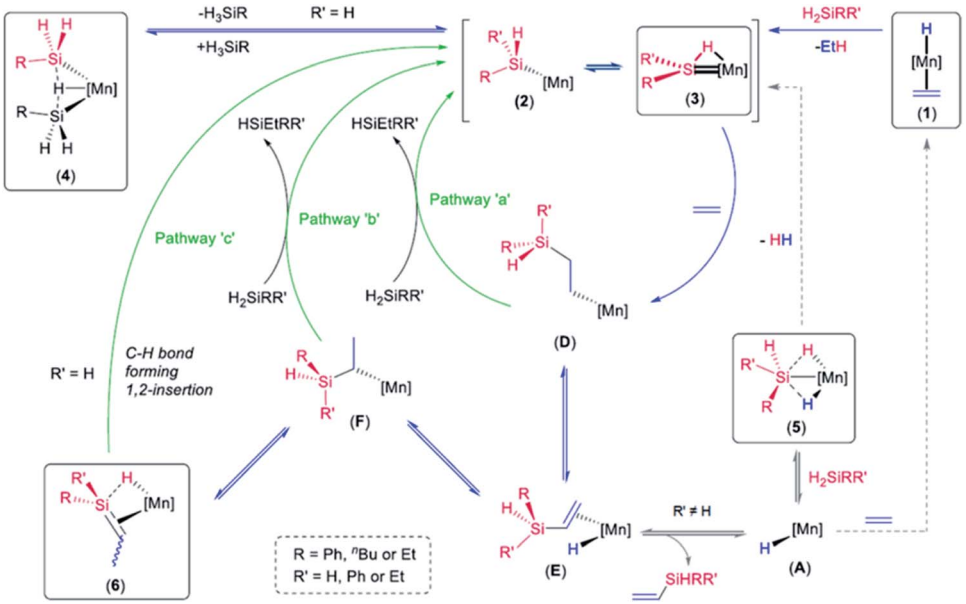

Scheme 8 Proposed catalytic cycle for ethylene hydrosilylation by primary and secondary hydrosilanes. [Mn] = $Mn(dmpe)_2$. Only one isomer is shown for complexes **3** and **5**. Boxes represent complexes observed by NMR spectroscopy during catalysis.

substrates: ethylene to form **1**, or hydrosilanes to form silyl dihydride complexes (**5**); Scheme 8. While **1** reacts with primary or secondary hydrosilanes (but not tertiary hydrosilanes) to generate ethane and low-coordinate silyl species **2**, complex **5** can slowly rejoin the catalytic cycle by H_2 elimination to afford **2**. Support for this H_2 elimination process was obtained experimentally at elevated temperatures. For example, heating a solution of $[(dmpe)_2MnH_2(SiH_2Ph)]$ ($\mathbf{5^{Ph}}$) under D_2 at 70–80 °C overnight resulted in >90% deuterium incorporation into the Mn*H* environments, exclusively. Furthermore, reactions of $\mathbf{5^{Bu}}$ with ^{t}BuNC, and $[(dmpe)_2MnD_2(SiH_2Ph)]$ ($\boldsymbol{d_2}$**_5^{Ph}**) with *o*-xylylNC, afforded $[(dmpe)_2Mn(SiH_2{}^nBu)(CN{}^tBu)]$ (**7d**) and $[(dmpe)_2Mn(SiH_2Ph)(CNXyl)]$ (**7a**), respectively, after 1 h at 75 °C.

In an effort to determine whether pathway 'a' (*via* primary alkyl intermediate **D**), 'b' (*via* secondary alkyl intermediate **F**), or 'c' (*via* a silene hydride complex with an Si*H* substituent; $\mathbf{6^{R,H}}$) in Scheme 8 is operative, catalysis was carried out using d_4-ethylene; pathway 'a' would generate CD_2CD_2H groups, whereas pathways 'b' and 'c' would generate $CHDCD_3$ groups.[69] Hydrosilylation of C_2D_4 by the secondary hydrosilane H_2SiEt_2 yielded d_4-$HSiEt_3$, primarily as $HSiEt_2(CD_2CD_2H)$ (97%), with a minor amount of $HSiEt_2(CDHCD_3)$ (3%), as determined by ^1H, ^2H, and $^{13}C\{^1H\}$ NMR analysis (Fig. S471†), indicating that pathway 'a' in Scheme 8 is dominant. By contrast, C_2D_4 hydrosilylation by H_3Si^nBu under identical conditions yielded a solution containing 20% $HSi^nBu(CD_2CD_2H)_2$, and 80% $HSi^nBu(CD_2CD_2H)(CDHCD_3)$. Given that H_2SiEt_2 has been shown to react almost exclusively *via* pathway 'a' (affording a CD_2CD_2H substituent on silicon), and H_2Si^nBuEt can be expected to react analogously, this product distribution indicates that H_3Si^nBu is converted to H_2Si^nBuEt primarily *via* pathway 'b' and/or 'c' (~77%), with a lesser contribution from pathway 'a' (~23%).

DFT calculations indicate that alkyl intermediates **D** and **F** are very similar in energy (within 5 kJ mol^{-1}). Therefore, the preferential reactivity of secondary silanes towards less hindered **D** (pathway 'a') may be sterically driven. By contrast, for conversion of primary to secondary hydrosilanes, where pathway 'b' and/or 'c' is dominant, it is not obvious why pathway 'b' would be preferred over pathway 'a'. Pathway 'c' is therefore a viable alternative, especially given that 'c' has been demonstrated (*vide supra*) in room temperature stoichiometric reactions involving silenes with a hydrogen substituent on silicon ($\mathbf{6^{R,H}}$). Furthermore, it is notable that silenes ($\mathbf{6^{R,H}}$) are the dominant metal-containing species during the first phase of catalysis (conversion of primary to secondary hydrosilanes).

Summary and conclusions

The disilyl hydride manganese complexes, $[(dmpe)_2MnH(SiH_2R)_2]$ (R = Ph or ^{n}Bu), reversibly dissociate H_3SiR to access low-coordinate silyl ($[(dmpe)_2Mn(SiH_2R)]$) and silylene hydride ($[(dmpe)_2MnH(=SiHR)]$) complexes. The *trans* isomers of the silylene hydride complexes were observed in small amounts (<5% relative to the disilyl hydride) by NMR spectroscopy at 333 K, and are the first spectroscopically observed examples of group 7 $L_xM{=}SiHR$ compounds. DFT calculations support the thermodynamic accessibility of *cis*- and *trans*-isomers of these low coordinate silyl and silylene species, and both sets of intermediates were trapped by coordination of isonitriles (to manganese) or N-heterocyclic carbenes (to silicon).

The reactivity of $[(dmpe)_2MnH(SiH_2R)_2]$ (R = Ph or ^{n}Bu) with ethylene was investigated, affording silene hydride complexes $[(dmpe)_2MnH(RHSi{=}CHMe)]$. This reaction represents a unique method to access silene complexes (analogous to reactions of ethylene with $[(dmpe)_2MnH(=SiR_2)]$ compounds in our previous

communication),[32] and the resulting silene complexes are the first transition metal examples with an Si*H* substituent. As such, they displayed unusual reactivity: for example, [(dmpe)$_2$MnH(RHSi=CHMe)] slowly converted to a more stable silylene hydride isomer, [(dmpe)$_2$MnH(=SiEtR)]; the first example of isomerization of a silene hydride complex to a silylene hydride complex. Furthermore, [(dmpe)$_2$MnH(RHSi=CHMe)] reacted with a second equivalent of ethylene to convert the Si*H* substituent to an Si*Et* substituent, which is an unprecedented transformation for a silene ligand.

All of the silyl, silylene and silene complexes in this work were accessed *via* reactions of [(dmpe)$_2$MnH(C_2H_4)] (**1**) with hydrosilanes and/or ethylene. Therefore, ethylene hydrosilylation was investigated using **1** as a pre-catalyst, resulting in stepwise conversion of primary to secondary to tertiary hydrosilanes. Manganese complexes observed during catalysis include (a) disilyl hydride complexes, (b) silylene hydride complexes, (c) silene hydride complexes, (d) silyl dihydride complexes, and (e) the ethylene hydride pre-catalyst. All of these species are catalytically active (although the silyl dihydride complexes are significantly less active than the others), and a catalytic cycle is proposed on the basis of these observations, the aforementioned stoichiometric reactions, and hydrosilylation of d_4-ethylene. This catalytic cycle is unusual due to the involvement of silylene hydride and silene hydride complexes, potentially as on-cycle species.

Conflicts of interest

There are no conflicts to declare.

Acknowledgements

D. J. H. E. thanks NSERC of Canada for a Discovery Grant. We are grateful to Dr Jim Britten of the McMaster Analytical X-ray Diffraction Facility, Dr Bob Berno and Hilary Jenkins of the McMaster NMR Facility, and Dr Ignacio Vargas-Baca of McMaster University Department of Chemistry for advice and support with X-ray diffraction, NMR spectroscopy, and DFT calculations respectively. We are also grateful to Dr Yurij Mozharivskyj and Fang Yuan for collection of X-ray diffraction data for **8b,c** while the department's diffractometer was out of commission. Also, we are grateful to Compute Canada for access to computational resources and Aathith Vasanthakumar for providing ^{iPr}NHC for the synthesis of **8a,b**.

Notes and references

1 (*a*) M. Weidenbruch, *Coord. Chem. Rev.*, 1994, **130**, 275–300; (*b*) P. Gaspar and R. West, in *The Chemistry of Organic Silicon Compounds*, ed. Z. Rappoport and Y. Apeloig, John Wiley & Sons, Chichester, UK, 1998, ch. 43, vol. 2, pp. 2463–2568; (*c*) P. P. Gaspar and D. Zhou, *Sci. Synth.*, 2002, **4**, 135–158.

2 M. Brook, in *Silicon in Organic, Organometallics, and Polymer Chemistry*, John Wiley & Sons, New York, 2000, ch. 3, pp. 39–96.

3 A. G. Brook and M. A. Brook, *Adv. Organomet. Chem.*, 1996, **39**, 71–158.

4 (*a*) T. Müller, W. Ziche and N. Auner, in *The Chemistry of Organic Silicon Compounds*, ed. Z. Rappoport and Y. Apeloig, John Wiley & Sons, Chichester, UK, 1998, ch. 16, vol. 2, pp. 857–1062; (*b*) K. M. Baines and M. S. Samuel, *Sci. Synth.*, 2002, **4**, 125–134; (*c*) H.-W. Lerner, *Recent Res. Dev. Org. Chem.*, 2004, **8**, 159–196; (*d*) H. Ottosson and P. G. Steel, *Chem.–Eur. J.*, 2006, **12**, 1576–1585; (*e*) H. Ottosson and A. M. Rouf, *Sci. Synth., Knowl. Updates*, 2011, 37–46.

5 (*a*) M. Haaf, T. A. Schmedake and R. West, *Acc. Chem. Res.*, 2000, **33**, 704–714; (*b*) B. Gehrhus and M. F. Lappert, *J. Organomet. Chem.*, 2001, **617–618**, 209–223; (*c*) N. J. Hill and R. West, *J. Organomet. Chem.*, 2004, **689**, 4165–4183; (*d*) Y. Mizuhata, T. Sasamori and N. Tokitoh, *Chem. Rev.*, 2009, **109**, 3479–3511; (*e*) T. Iwamoto and S. Ishida, in *Organosilicon Compounds: Theory and Experiment (Synthesis)*, ed. V. Y. Lee, Academic Press, London, 2017, ch. 8, vol. 1, pp. 361–532; (*f*) K. M. Baines, *Chem. Commun.*, 2013, **49**, 6366–6369.

6 (*a*) P. D. Lickiss, *Chem. Soc. Rev.*, 1992, **21**, 271–279; (*b*) H. Ogino, *Chem. Rec.*, 2002, **2**, 291–306.

7 M. Okazaki, H. Tobita and H. Ogino, *Dalton Trans.*, 2003, 493–506.

8 R. Waterman, P. G. Hayes and T. D. Tilley, *Acc. Chem. Res.*, 2007, **40**, 712–719.

9 Y. Tian, W. Zhang, M. Ge, S. Yu, X. Lv and T. Zhang, *RSC Adv.*, 2016, **6**, 21048–21055.

10 L. J. Procopio and D. H. Berry, *J. Am. Chem. Soc.*, 1991, **113**, 4039–4040.

11 P. I. Djurovich, A. R. Dolich and D. H. Berry, *J. Chem. Soc., Chem. Commun.*, 1994, 1897–1898.

12 D. H. Berry and L. J. Procopio, *J. Am. Chem. Soc.*, 1989, **111**, 4099–4100.

13 P. I. Djurovich, P. J. Carroll and D. H. Berry, *Organometallics*, 1994, **13**, 2551–2553.

14 H. Fang, W. Hou, G. Liu and Z. Huang, *J. Am. Chem. Soc.*, 2017, **139**, 11601–11609.

15 Y. Shi, *Acc. Chem. Res.*, 2015, **48**, 163–173.

16 (*a*) G. Schmid and E. Welz, *Angew. Chem., Int. Ed. Engl.*, 1977, **16**, 785–786; (*b*) D. A. Straus, T. D. Tilley, A. L. Rheingold and S. J. Geib, *J. Am. Chem. Soc.*, 1987, **109**, 5872–5873; (*c*) C. Zybill and G. Müller, *Angew. Chem., Int. Ed. Engl.*, 1987, **26**, 669–670.

17 D. A. Straus, S. D. Grumbine and T. D. Tilley, *J. Am. Chem. Soc.*, 1990, **112**, 7801–7802.

18 A handful of base-free silylene complexes involving group 4 or 5 transition metals have also been reported (*a*) A. V. Lalov, M. P. Egorov, O. M. Nefedov, V. K. Cherkasov, N. L. Ermolaev and A. V. Piskunov, *Russ. Chem. Bull.*, 2005, **54**, 807–810; (*b*) N. Nakata, T. Fujita and A. Sekiguchi, *J. Am. Chem. Soc.*, 2006, **128**, 16024–16025; (*c*) A. Shinohara, J. McBee, R. Waterman and T. D. Tilley, *Organometallics*, 2008, **27**, 5717–5722; (*d*) B. Blom, M. Driess, D. Gallego and S. Inoue, *Chem.–Eur. J.*, 2012, **18**, 13355–13360; (*e*) R. Azhakar, R. S. Ghadwal, H. W. Roesky, J. Hey and D. Stalke, *Chem.–Asian J.*, 2012, **7**,

528–533; (*f*) V. Y. Lee, S. Aoki, T. Yokoyama, S. Horiguchi, A. Sekiguchi, H. Gornitzka, J.-D. Guo and S. Nagase, *J. Am. Chem. Soc.*, 2013, **135**, 2987–2990.

19 R. S. Simons, J. C. Gallucci, C. A. Tessier and W. J. Youngs, *J. Organomet. Chem.*, 2002, **654**, 224–228.

20 J. D. Feldman, J. C. Peters and T. D. Tilley, *Organometallics*, 2002, **21**, 4065–4075.

21 T. Watanabe, H. Hashimoto and H. Tobita, *Angew. Chem., Int. Ed.*, 2004, **43**, 218–221.

22 B. V. Mork, T. D. Tilley, A. J. Schultz and J. A. Cowan, *J. Am. Chem. Soc.*, 2004, **126**, 10428–10440.

23 (*a*) E. Calimano and T. D. Tilley, *J. Am. Chem. Soc.*, 2008, **130**, 9226–9227; (*b*) E. Calimano and T. D. Tilley, *J. Am. Chem. Soc.*, 2009, **131**, 11161–11173; (*c*) T. Fukuda, T. Yoshimoto, H. Hashimoto and H. Tobita, *Organometallics*, 2016, **35**, 921–924; (*d*) P. B. Glaser and T. D. Tilley, *J. Am. Chem. Soc.*, 2003, **125**, 13640–13641.

24 (*a*) B. V. Mork and T. D. Tilley, *J. Am. Chem. Soc.*, 2004, **126**, 4375–4385; (*b*) T. Fukuda, H. Hashimoto, S. Sakaki and H. Tobita, *Angew. Chem., Int. Ed.*, 2016, **55**, 188–192; (*c*) P. B. Glaser and T. D. Tilley, *Organometallics*, 2004, **23**, 5799–5812; (*d*) P. G. Hayes, C. Beddie, M. B. Hall, R. Waterman and T. D. Tilley, *J. Am. Chem. Soc.*, 2006, **128**, 428–429; (*e*) M. Ochiai, H. Hashimoto and H. Tobita, *Angew. Chem., Int. Ed.*, 2007, **46**, 8192–8194; (*f*) P. G. Hayes, R. Waterman, P. B. Glaser and T. D. Tilley, *Organometallics*, 2009, **28**, 5082–5089; (*g*) M. E. Fasulo, P. B. Glaser and T. D. Tilley, *Organometallics*, 2011, **30**, 5524–5531.

25 (*a*) T. Yoshimoto, H. Hashimoto, N. Hayakawa, T. Matsuo and H. Tobita, *Organometallics*, 2016, **35**, 3444–3447; (*b*) M. E. Fasulo, M. C. Lipke and T. D. Tilley, *Chem. Sci.*, 2013, **4**, 3882–3887.

26 (*a*) H.-J. Liu, C. Raynaud, O. Eisenstein and T. D. Tilley, *J. Am. Chem. Soc.*, 2014, **136**, 11473–11482; (*b*) P. W. Smith and T. D. Tilley, *J. Am. Chem. Soc.*, 2018, **140**, 3880–3883.

27 Pt and Ni silene complexes have been reported featuring coordination to a stabilized silene (*a*) D. Bravo-Zhivotovskii, H. Peleg-Vasserman, M. Kosa, G. Molev, M. Botoshanskii and Y. Apeloig, *Angew. Chem., Int. Ed.*, 2004, **43**, 745–748; (*b*) N. Nakata, R. Rodriguez, T. Troadec, N. Saffon-Merceron, J.-M. Sotiropoulos, A. Baceiredo and T. Kato, *Angew. Chem., Int. Ed.*, 2013, **52**, 10840–10844.

28 S. R. Klei, T. D. Tilley and R. G. Bergman, *Organometallics*, 2001, **20**, 3220–3222.

29 (*a*) B. K. Campion, R. H. Heyn and T. D. Tilley, *J. Am. Chem. Soc.*, 1990, **112**, 4079–4081; (*b*) B. K. Campion, R. H. Heyn, T. D. Tilley and A. L. Rheingold, *J. Am. Chem. Soc.*, 1993, **115**, 5527–5537; (*c*) B. K. Campion, R. H. Heyn and T. D. Tilley, *J. Am. Chem. Soc.*, 1988, **110**, 7558–7560.

30 (*a*) V. K. Dioumaev, P. J. Carroll and D. H. Berry, *Angew. Chem., Int. Ed.*, 2003, **42**, 3947–3949; (*b*) T. S. Koloski, P. J. Carroll and D. H. Berry, *J. Am. Chem. Soc.*, 1990, **112**, 6405–6406.

31 (*a*) G. S. Girolami, G. Wilkinson, M. Thornton-Pett and M. B. Hursthouse, *J. Am. Chem. Soc.*, 1983, **105**, 6752–6753; (*b*) G. S. Girolami, C. G. Howard, G. Wilkinson, H. M. Dawes, M. Thornton-Pett, M. Motevalli and M. B. Hursthouse, *J. Chem. Soc., Dalton Trans.*, 1985, 921–929.

32 J. S. Price, D. J. H. Emslie and J. F. Britten, *Angew. Chem., Int. Ed.*, 2017, **56**, 6223–6227.

33 A variety of other Mo silylene hydride complexes have been reported to feature Si–H interligand interactions, but for these complexes an X-ray crystal structure was not obtained, or the bridging hydride was not located from the difference map.

34 (*a*) M. C. Lipke, F. Neumeyer and T. D. Tilley, *J. Am. Chem. Soc.*, 2014, **136**, 6092–6102; (*b*) V. M. Iluc and G. L. Hillhouse, *J. Am. Chem. Soc.*, 2010, **132**, 11890–11892; (*c*) T. Watanabe, H. Hashimoto and H. Tobita, *Chem.–Asian J.*, 2012, **7**, 1408–1416.

35 J. S. Price, D. J. H. Emslie, I. Vargas-Baca and J. F. Britten, *Organometallics*, 2018, **37**, 3010–3023.

36 J. S. Price, D. J. H. Emslie and B. Berno, *Organometallics*, 2019, **38**, 2347–2362.

37 A. K. Roy, *Adv. Organomet. Chem.*, 2008, **55**, 1–59.

38 D. Troegel and J. Stohrer, *Coord. Chem. Rev.*, 2011, **255**, 1440–1459.

39 (*a*) Y. Nakajima and S. Shimada, *RSC Adv.*, 2015, **5**, 20603–20616; (*b*) M. C. Lipke, A. L. Liberman-Martin and T. D. Tilley, *Angew. Chem., Int. Ed.*, 2017, **56**, 2260–2294; (*c*) M. Brook, in *Silicon in Organic, Organometallics, and Polymer Chemistry*, John Wiley & Sons, New York, 2000, pp. 401–422.

40 D. A. Valyaev, G. Lavigne and N. Lugan, *Coord. Chem. Rev.*, 2016, **308**, 191–235.

41 X. Yang and C. Wang, *Chem.–Asian J.*, 2018, **13**, 2307–2315.

42 (*a*) S. L. Pratt and R. A. Faltynek, *J. Organomet. Chem.*, 1983, **258**, C5–C8; (*b*) H. S. Hilal, M. Abu-Eid, M. Al-Subu and S. Khalaf, *J. Mol. Catal.*, 1987, **39**, 1–11; (*c*) H. S. Hilal, M. A. Suleiman, W. J. Jondi, S. Khalaf and M. M. Masoud, *J. Mol. Catal. A: Chem.*, 1999, **144**, 47–59; (*d*) J. H. Docherty, J. Peng, A. P. Dominey and S. P. Thomas, *Nat. Chem.*, 2017, **9**, 595–600; (*e*) T. K. Mukhopadhyay, M. Flores, T. L. Groy and R. J. Trovitch, *Chem. Sci.*, 2018, **9**, 7673–7680; (*f*) X. Yang and C. Wang, *Chin. J. Chem.*, 2018, **36**, 1047–1051; (*g*) J. R. Carney, B. R. Dillon, L. Campbell and S. P. Thomas, *Angew. Chem., Int. Ed.*, 2018, **57**, 10620–10624.

43 B. Marciniec, H. Maciejewski, C. Pietraszuk and P. Pawluć, *Hydrosilylation: A Comprehensive Review on Recent Advances*, Springer, Netherlands, 2009.

44 Over the 4 days that this reaction was monitored by ^{1}H NMR spectroscopy, the ethylene concentration in solution decreased by 40%. Relative concentrations in Fig. 2 were calculated by integrating ^{1}H NMR data; integration relative to the residual solvent signal from C_6D_6 indicated that the total moles of manganese-containing species in the inset in Fig. 2 remained constant.

45 In the reaction of $\mathbf{4^{Ph}}$ with ethylene, no tertiary hydrosilane was observed. However, small amounts of a vinyl hydrosilane were observed.

46 DFT calculations indicated that isomerization of Si*H*-containing silene hydride complexes $\mathbf{6^{R,H}}$ to silylene hydride complexes *trans*-[(dmpe)$_2$MnH(=SiEtR)] (***trans***-

$\mathbf{3^{R,Et}}$) is thermodynamically favourable for R = Ph and ^{n}Bu; minima for the latter complexes were located 20–34 kJ mol^{-1} lower in energy than the lowest energy silene hydride isomer. In addition, *cis* silylene hydride isomers were determined to be 1 ($\mathbf{3^{Ph,Et}}$) and 9 ($\mathbf{3^{Bu,Etb}}$) kJ mol^{-1} less stable than the respective *trans* isomers.

47 NMR data for *trans*-[(dmpe)$_2$MnH(=SiEt$_2$)] (***trans*-3^{Et2}**) includes an Mn*H* ^{1}H NMR peak at −10.46 ppm (quintet with $^{2}J_{H,P}$ of 51 Hz), a single sharp singlet in the ^{31}P{^{1}H} NMR spectrum at 80.95 ppm, and a ^{29}Si NMR chemical shift of 365 ppm; see ref. 32.

48 Iron or cobalt silene complexes with hydrogen substituents on Si have been detected in the gas phase by mass spectrometry and postulated as an intermediate in the gas-phase activation of H_3SiEt by Co cations; (*a*) R. Bakhtiar, C. M. Holznagel and D. B. Jacobson, *J. Am. Chem. Soc.*, 1993, **115**, 345–347; (*b*) D. B. Jacobson and R. Bakhtiar, *J. Am. Chem. Soc.*, 1993, **115**, 10830–10844; (*c*) S. Bärsch, T. Böhme, D. Schröder and H. Schwarz, *Int. J. Mass Spectrom.*, 2000, **199**, 107–125.

49 Not including enantiomers where the stereochemistry at manganese is switched from Λ to Δ.

50 The dominant isomer for $\mathbf{6^{Bu,H}}$ was assigned as isomer i given that the Si*H* ^{1}H NMR signal for this isomer exhibits a large (18 Hz) $^{3}J_{^{1}H,^{31}P}$ coupling to one of the phosphorus donor atoms, and in the calculated structures of isomers (i) and (ii) (for a model of $\mathbf{6^{Bu,H}}$ where the ^{n}Bu group was replaced with an Et group), only isomer (i) exhibited a ^{1}H–^{31}P coupling of comparable magnitude (23 Hz). As well, isomer i of $\mathbf{6^{Bu,H}}$ is slightly (4 kJ mol^{-1}) lower in energy than isomer (ii).

51 C. R. Groom, I. J. Bruno, M. P. Lightfoot and S. C. Ward, *Acta Crystallogr., Sect. B: Struct. Sci., Cryst. Eng. Mater.*, 2016, **72**, 171–179.

52 By comparison, terminal Si–H distances and Mayer bond orders in $\mathbf{6^{R,H}}$ are 1.50–1.51 Å and 0.82–0.86, respectively.

53 (*a*) S. K. Ignatov, N. H. Rees, B. R. Tyrrell, S. R. Dubberley, A. G. Razuvaev, P. Mountford and G. I. Nikonov, *Chem.–Eur. J.*, 2004, **10**, 4991–4999; (*b*) P. Meixner, K. Batke, A. Fischer, D. Schmitz, G. Eickerling, M. Kalter, K. Ruhland, K. Eichele, J. E. Barquera-Lozada, N. P. M. Casati, F. Montisci, P. Macchi and W. Scherer, *J. Phys. Chem. A*, 2017, **121**, 7219–7235.

54 In the case of $\mathbf{4^{Ph}}$, an additional low frequency ^{1}H NMR signal (a broad singlet with <2% intensity relative to the Mn*H* peak of $\mathbf{4^{Ph}}$) was observed at −12.1 ppm (335 K), which could potentially be from the Mn*H* environment of *cis*-[(dmpe)$_2$MnH(=SiHPh)] (***cis*-3^{Ph,H}**). However, EXSY NMR spectroscopy did not show chemical exchange between this peak and those from $\mathbf{4^{Ph}}$ or ***trans*-3^{Ph,H}** (potentially due to broadness and low intensity of the signal). A further low frequency ^{1}H NMR signal (also a broad singlet, but present in the room temperature and high temperature NMR spectra in similar intensities; ∼1.5% relative to the Mn*H* region of $\mathbf{4^{Ph}}$) was observed at −13.8 ppm, which could potentially be from another isomer of $\mathbf{4^{Ph}}$; this environment was observed by EXSY NMR spectroscopy to be in chemical exchange with the Si*H* and Mn*H* environments of both $\mathbf{4^{Ph}}$ and ***trans*-3^{Ph,H}**.

55 (*a*) R. S. Ghadwal, R. Azhakar, K. Pröpper, J. J. Holstein, B. Dittrich and H. W. Roesky, *Inorg. Chem.*, 2011, **50**, 8502–8508; (*b*) A. C. Filippou, B. Baars, O. Chernov, Y. N. Lebedev and G. Schnakenburg, *Angew. Chem., Int. Ed.*, 2014, **53**, 565–570; (*c*) R. S. Ghadwal, D. Rottschäfer, D. M. Andrada, G. Frenking, C. J. Schürmann and H.-G. Stammler, *Dalton Trans.*, 2017, **46**, 7791–7799; (*d*) M. Majumdar, I. Omlor, C. B. Yildiz, A. Azizoglu, V. Huch and D. Scheschkewitz, *Angew. Chem., Int. Ed.*, 2015, **54**, 8746–8750; (*e*) S. M. I. Al-Rafia, A. C. Malcolm, R. McDonald, M. J. Ferguson and E. Rivard, *Chem. Commun.*, 2012, **48**, 1308–1310; (*f*) C. Eisenhut, T. Szilvási, G. Dübek, N. C. Breit and S. Inoue, *Inorg. Chem.*, 2017, **56**, 10061–10069; (*g*) T. Fukuda, H. Hashimoto and H. Tobita, *J. Am. Chem. Soc.*, 2015, **137**, 10906–10909; (*h*) D. Lutters, C. Severin, M. Schmidtmann and T. Müller, *J. Am. Chem. Soc.*, 2016, **138**, 6061–6067; (*i*) H. P. Hickox, Y. Wang, Y. Xie, P. Wei, H. F. Schaefer III and G. H. Robinson, *J. Am. Chem. Soc.*, 2016, **138**, 9799–9802; (*j*) H. Zhang, Z. Ouyang, Y. Liu, Q. Zhang, L. Wang and L. Deng, *Angew. Chem., Int. Ed.*, 2014, **53**, 8432–8436; (*k*) H. Schneider, D. Schmidt, A. Eichhöfer, M. Radius, F. Weigend and U. Radius, *Eur. J. Inorg. Chem.*, 2017, **2017**, 2600–2616; (*l*) A. Maiti, D. Mandal, I. Omlor, D. Dhara, L. Klemmer, V. Huch, M. Zimmer, D. Scheschkewitz and A. Jana, *Inorg. Chem.*, 2019, **58**, 4071–4075; (*m*) J. Li, S. Merkel, J. Henn, K. Meindl, A. Döring, H. W. Roesky, R. S. Ghadwal and D. Stalke, *Inorg. Chem.*, 2010, **49**, 775–777; (*n*) G. Tavcar, S. S. Sen, R. Azhakar, A. Thorn and H. W. Roesky, *Inorg. Chem.*, 2010, **49**, 10199–10202; (*o*) R. J. Witzke and T. D. Tilley, *Chem. Commun.*, 2019, **55**, 6559–6562.

56 A handful of NHC-stabilized silylene complexes have also been reported with ^{29}Si chemical shifts lower than 25 ppm (see ref. 55*e–h*), and this has been rationalized by adoption of a zwitterionic bonding motif which results in limited π-backdonation to the Si center from the metal (see ref. 55*h*).

57 We could not determine the ^{29}Si NMR chemical shift of ***trans*-8c** due to the low proportion of trans isomer in solution (*cis* : *trans* ratio of 14 : 1).

58 The lability of NHCs in **8a–d** was also illustrated by initial generation of mixtures of reagents and products upon addition of free NHCs to $\mathbf{4^{R}}$; complete conversion to **8a–d** required removal of the free hydrosilane byproducts. For **8b–d**, this was achieved by periodically removing all solvent and hydrosilane byproducts *in vacuo*. By contrast, for **8a** this was achieved by the reaction of the H_3SiPh byproduct with excess ^{iPr}NHC to form 1-phenyl-2,5-diisopropyl-3,4-dehydro-2,5-diazasilinane; this reaction has previously been reported at 100 °C, and in our hands 98% conversion was observed after 24 h at 55 °C (consistent with the reaction conditions involved in the synthesis of **8a**). D. Schmidt, J. Berthel, S. Pietsch and U. Radius, *Angew. Chem., Int. Ed.*, 2012, **51**, 8881–8885.

59 Unlike the reaction of $\mathbf{4^{Bu}}$ with ethylene, the reaction of **8b** with ethylene does not generate $H_3Si^{n}Bu$ as a byproduct,

and under these conditions, complex $\mathbf{6}^{\mathbf{Bu,H}}$ reacted readily with a further equivalent of ethylene, so that both $\mathbf{6}^{\mathbf{Bu,H}}$ and $\mathbf{6}^{\mathbf{Bu,Et}}$ were formed concurrently.

60 In the structures of ***cis*-8a,b**, the dmpe ligands are disordered, and modelling this disorder allowed the structures of both diastereomers observed in solution to be elucidated.

61 **7b**,**d** were computationally modelled with Et groups in place of ^{n}Bu groups; [(dmpe)$_2$Mn(SiH$_2$Et)(CNR)] (**7b***: R = *o*-xylyl, **7d***: R = ^{t}Bu).

62 Alternative pathways requiring initial dissociation of a phosphine donor in $\mathbf{6}^{\mathbf{R,H}}$ followed by ethylene coordination (with subsequent oxidative coupling or 1,2-insertion reactivity) cannot be ruled out.

63 Silylene complexes were only observed during catalysis when most of the ethylene had been consumed.

64 C. J. Kong, S. E. Gilliland III, B. R. Clark and B. F. Gupton, *Chem. Commun.*, 2018, **54**, 13343–13346.

65 For examples of ethylene hydrosilylation selective for producing secondary hydrosilanes, see ref. 23*d* and (*a*) T. I. Gountchev and T. D. Tilley, *Organometallics*, 1999, **18**, 5661–5667. For examples of ethylene hydrosilylation selective for producing quaternary silanes, see (*b*) L. A. Oro, M. J. Fernandez, M. A. Esteruelas and M. S. Jimenez, *J. Mol. Catal.*, 1986, **37**, 151–156; (*c*) R. S. Tanke and R. H. Crabtree, *Organometallics*, 1991, **10**, 415–418; (*d*) S. Lachaize, S. Sabo-Etienne, B. Donnadieu and B. Chaudret, *Chem. Commun.*, 2003, 214–215; (*e*) E. A. Chernyshev, Z. V. Belyakova, S. P. Knyazev, G. N. Turkel'taub, E. V. Parshina, I. V. Serova and P. A. Storozhenko, *Russ. J. Gen. Chem.*, 2006, **76**, 225–228; (*f*) J. J. Adams, N. Arulsamy and D. M. Roddick, *Organometallics*, 2009, **28**, 1148–1157; (*g*) S. Lachaize, L. Vendier and S. Sabo-Etienne, *Dalton Trans.*, 2010, **39**, 8492–8500.

66 M. A. Schroeder and M. S. Wrighton, *J. Organomet. Chem.*, 1977, **128**, 345–358.

67 Energy minima for alkyl intermediates **D** and **F** were found to lie 46–67 kJ mol^{-1} higher in energy than the respective silene hydride resting states, indicating their thermodynamic accessibility from complexes observed by solution NMR spectroscopy.

68 In hydrosilylation reactions with d_4-ethylene, the vinyl byproducts contain fully deuterated vinyl groups, in keeping with the proposed pathway for their formation.

69 Hydrosilylation reactions involving C_2D_4 (with either $H_3Si^{n}Bu$ or H_2SiEt_2) proceeded to completion (*i.e.* complete consumption of the secondary hydrosilane reagent/intermediate) after 4 days at 60 °C, while analogous reactions using a higher pressure of C_2H_4 still contained 6–7% of the secondary hydrosilane ($H_2SiEt^{n}Bu$ intermediate or H_2SiEt_2 reagent), suggestive of an inverse kinetic isotope effect.